A Publication of the
Department of Geology
Brigham Young University
Provo, Utah 84602

Editors

Bart J. Kowallis
Karen Seely

Brigham Young University Geology Studies is published by the Department of Geology. This publication consists of graduate student and faculty research within the department as well as papers submitted by outside contributors. Each article submitted is externally reviewed by at least two qualified persons.

ISSN 0068-1016
2-93 600 2157

BRIGHAM YOUNG UNIVERSITY GEOLOGY STUDIES

Volume 39, 1993

CONTENTS

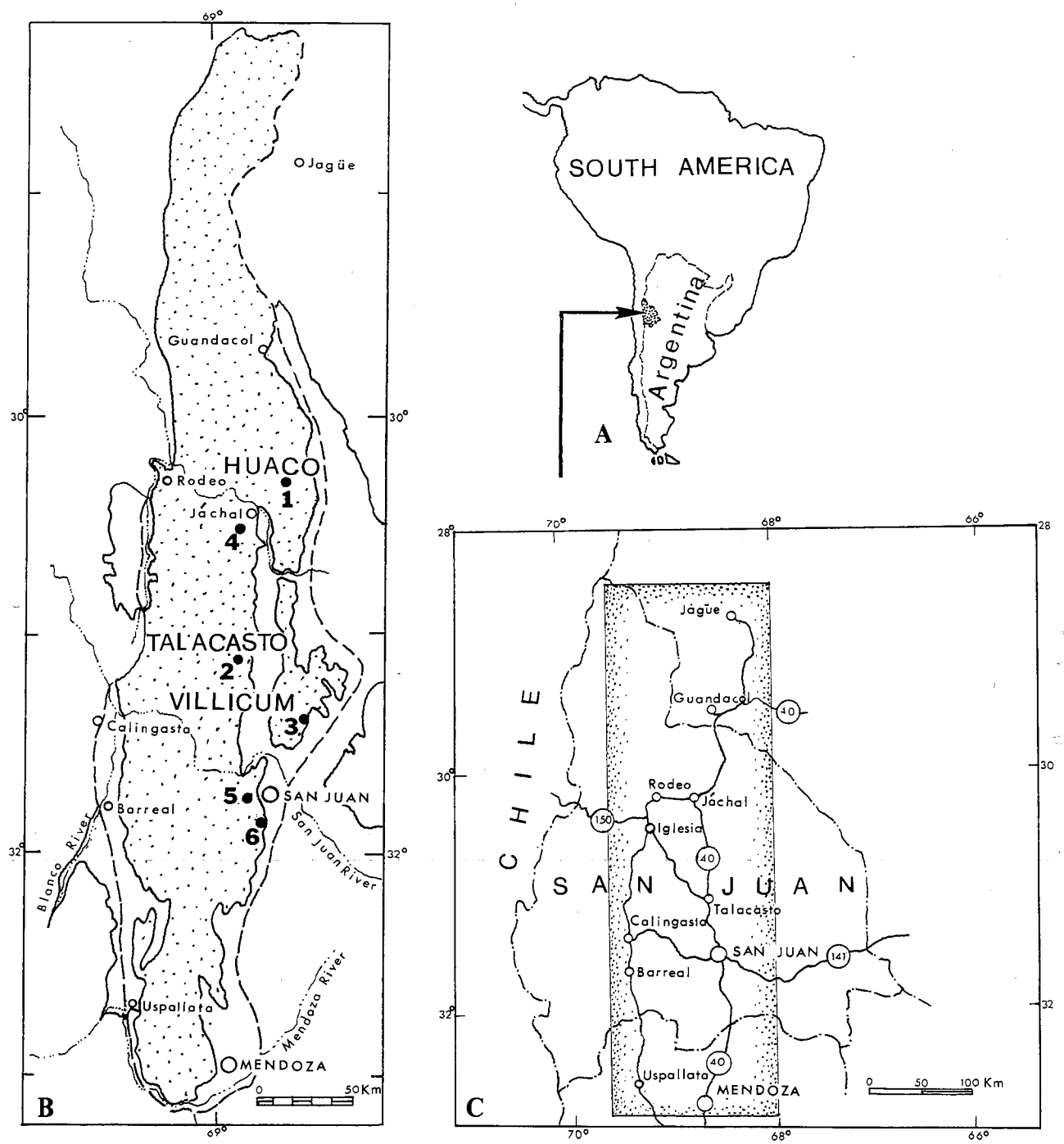

FIGURE 1.—*Index map to Ordovician sponge localities in Argentina. A—South America showing the position of the province of San Juan within Argentina (arrow). B—Sponge localities within the Precordillera (stippled) of central San Juan Province. Major localities (1–3) include: 1, the Huaco locality along sulfurous Agua Hedionda Creek, 30 miles east of Jáchal City; 2, Talacasto Gulch section in the Precordillera Central, approximately 89 km northwest of San Juan City; 3, Don Braulio Gulch in the Villicúm Range, approximately 40 km northwest of San Juan City. Other minor localities (4–6) include: 4, Loma del Piojo at San Roque Hill; 5, Las Lajas Gulch, west of San Juan City; 6, La Flecha Gulch in the Chica de Zonda Range, south of San Juan City. C—Map of San Juan Province showing the position of map B in the central part of the province.*

The Lower Ordovician Fillmore Formation of Western Utah: Storm-dominated Sedimentation on a Passive Margin

BENJAMIN F. DATTILO
Department of Geology, University of Cincinnati, Cincinnati, Ohio 45221-0013

ABSTRACT

A 94-m-thick section of the Lower Ordovician Fillmore Formation in the southern House Range of western Utah consists of shallow (50 m) subtidal through intertidal storm-deposited and fair-weather sediments arranged in shoaling-upward cycles of several scales deposited on a passive continental margin. Intermediate scale, 4–14-m-thick cycles consist of basal shelf shales interbedded with distal (offshore, near storm wave base) storm calcisiltites and trilobite-dominated flat-pebble conglomerates. These flat-pebble conglomerate packstones and grainstones commonly bear megaripples and are bimodally imbricated, suggesting they were formed by oscillating currents parallel to the trend of the Ibex basin and perpendicular to the shoreline. Each bed represents one or more storm events during which pebbles were ripped up and redeposited, then covered with fine sediment deposited from suspension as currents waned. These basal beds grade upward through intermediate-depth, wavy-laminated lime mudstone interbedded with calcisiltites and trilobite-dominated flat-pebble conglomerate packstones and grainstones with the addition of proximal encrinite-dominated flat-pebble conglomerate grainstones. The cycles are capped by algal-bound lime mudstones or lime mudstone mounds with hardgrounds that are iron-stained, probably by a limonite-weathering product of pyrite. These are capped by coarse encrinite grainstones with iron-stained intraclasts, which are shallow-water reworked storm deposits.

INTRODUCTION

Several studies of part or all of the Fillmore Formation have been undertaken since it was first named by Hintze (1951). Although many comments and observations have been made as to the environmental significance of various features and lithologies within the formation, to date no comprehensive depositional model for the Fillmore has been proposed, nor have general environments of deposition been delineated.

This project was undertaken to produce a depositional model based on detailed study of part of the Fillmore Formation in western Utah. As description and interpretation progressed, it became apparent that the storm depositional model, expounded by Aigner (1985) and slightly modified here, best explains Fillmore lithology and bedding.

This paper describes and discusses the salient features of Fillmore lithologies through detailed descriptions of microfacies analysis, sedimentary structures, and fossils. The depositional model is discussed in terms of these descriptions.

LOCATION AND STRATIGRAPHY

Sections for the study are located in the Fillmore outcrop area of the southern House Range of Millard County, western Utah (fig. 1). Five stratigraphic sections were measured in sections 30 and 31 (unsurveyed), T. 20 S, R. 13 W, and sections 25 (unsurveyed) and 36, T. 20 S, R. 14 W, in the Notch Peak Quadrangle. The study area is located 84 km (52 miles) southwest of Delta, Utah, and approximately 1.5 km (1 mile) north of U.S. 50-6 (figs. 1 and 2).

The Fillmore Formation lies in the lower part of the Pogonip Group, between the House Limestone and Wah Wah Limestone. It averages 500–550 m thick and crops out over an area of about 65 km^2 in the Notch Peak and the Barn 15-Minute Quadrangles (Hintze 1974a and 1974b). The present study concerns 94 m of the formation in trilobite zone G-2 (Hintze 1951), the *Macerodus dianae–Acodus deltatus* conodont interval of Ethington and Clark (1981), and parts of graptolite zones 1 and 2 of Braithwaite (1976). It is in the informal slope-forming shaly siltstone, light gray ledge-forming, and brown slope and ledge

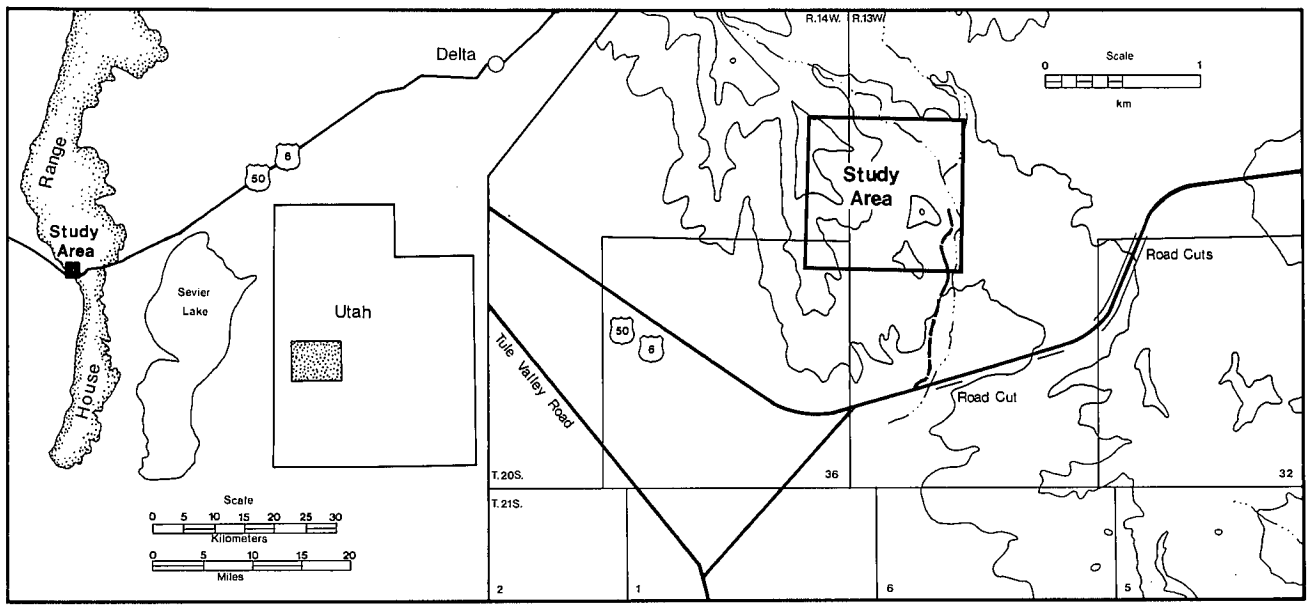

FIGURE 1.—*Index map of the study area in the southern House Range, Millard County, Utah. Base map is Notch Peak 15-Minute Quadrangle, United States Geological Survey.*

members of Hintze (1973) (figs. 3 and 4). The bottom of this interval is approximately 218 m above the base of the Fillmore Formation and extends from 33 m below to 61 m above a patch-reef horizon described by Church (1974).

GEOLOGIC SETTING

The study area lies in the Ibex basin, an intrashelf basin on a Cambro-Ordovician passive continental margin (Stewart and Poole 1974). The Fillmore Formation is part of the Ordovician shale and limestone facies, where deeper-water shale facies, to the west, intertongue with shallower limestone facies, to the east. The formation is mostly shale, with thin to very thin beds of flat-pebble conglomerate and calcisiltite-calcarenite limestone and thicker beds and mounds of lime mudstone.

METHODS

Five sections, 50 to 100 m thick, were measured using a Jacob's staff over an area of approximately 1/2 km^2 (fig. 2). Units 0.1 to 2 m thick were differentiated, based on parting planes and lithology, and these units were correlated, partly by walking and sighting between sections, to determine lateral variations in lithology.

Section 1 (figs. 2 and 4) was selected for more detailed study because of its accessibility and lack of faulting. Covered intervals were excavated, and notes were taken with the aid of a checklist (lithology, unit geometry, evidence of current directions, sedimentary structures, fossils, etc.) to insure consistency and completeness of each unit description. Other sections were described in terms of lithology and large-scale features alone.

At least one sample was collected within every 1-m interval in section 1 to insure a representative sampling of the entire section. Unusual lithologies, as well as fossils, were also collected.

More than 100 acetate peels were prepared from lithologic samples. A few thin sections of representative and unusual carbonate samples were also prepared. Samples,

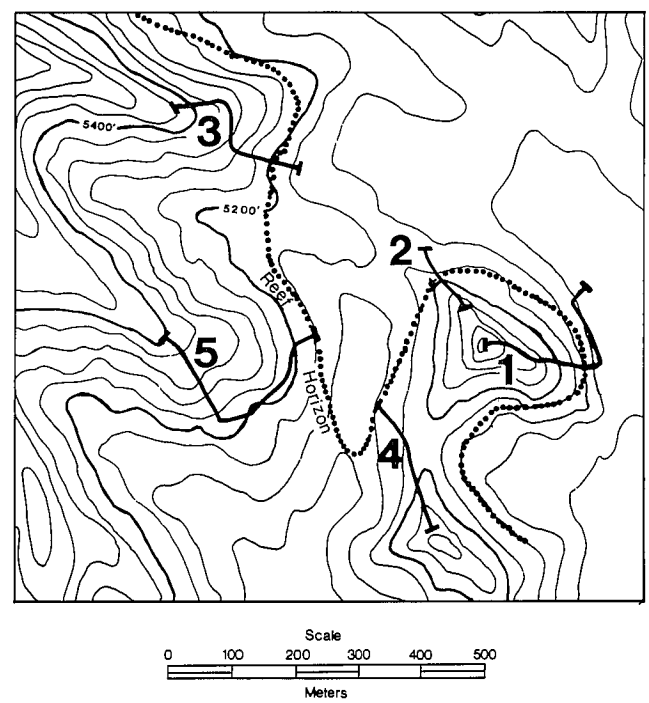

FIGURE 2.—*Detailed map shows locations of measured sections.*

peels, and thin sections were examined, and microfacies assignments were made using categories of Wilson (1975). Fossil content and diagenesis were also determined for characteristic lithologies; fossils collected were identified to genus where possible.

ACKNOWLEDGMENTS

This research was supported in part by a grant from the Associated Students of Brigham Young University, and in part through the Glen Nielson Fellowship, awarded through the Brigham Young University Department of Geology during the 1987–88 school year. I am indebted to Dr. R. L. Ethington, who identified conodont specimens, and to Dr. J. Keith Rigby, thesis chair, who aided in identification of sponges and provided editorial and technical advice.

MICROFACIES DESCRIPTIONS

OVERVIEW

Rocks of section 1 were divided into six major categories, each discussed below. The relative abundance of each rock type category is (1) shale, 44%; (2) wavy-laminated lime mudstone, 21%; (3) dense lime mudstone, 6%; (4) reef lime mudstone, less than 1%; (5) calcisiltite-calcarenite, 7%; and (6) flat-pebble conglomerate, 21% (trilobite-dominated, 16%). Hardgrounds are treated as an additional lithology. When specific examples are given from section 1, the reader may refer to figures 4 and 35 for stratigraphic position.

SHALE

Description

Calcareous shale is medium gray to olive gray and occurs both as thin partings between flat-pebble conglomerates and as very thick units. It generally splits irregularly, but certain intervals split evenly. Small slickensides are abundant and resulted from differential compaction.

Fossils

Body fossils. The shale fauna is diverse and is dominated by graptolites, orthocone nautiloids, small inarticulate brachiopods, and asaphid and pliomerid trilobites; echinoderm fragments are absent.

The subcylindrical sponge *Calycocoelia* is not a common faunal element but is restricted to shale. The cylindrical erect form of this sponge, as suggested by Wilson (1975), is probably an adaptation to faster sedimentation rates.

A *Loxonema*-like gastropod is also found commonly in shale along with two more rare forms resembling *Seelyia* and *Plethospira* (figs. 5B, D, E). *Macluritella* (fig. 5C) is

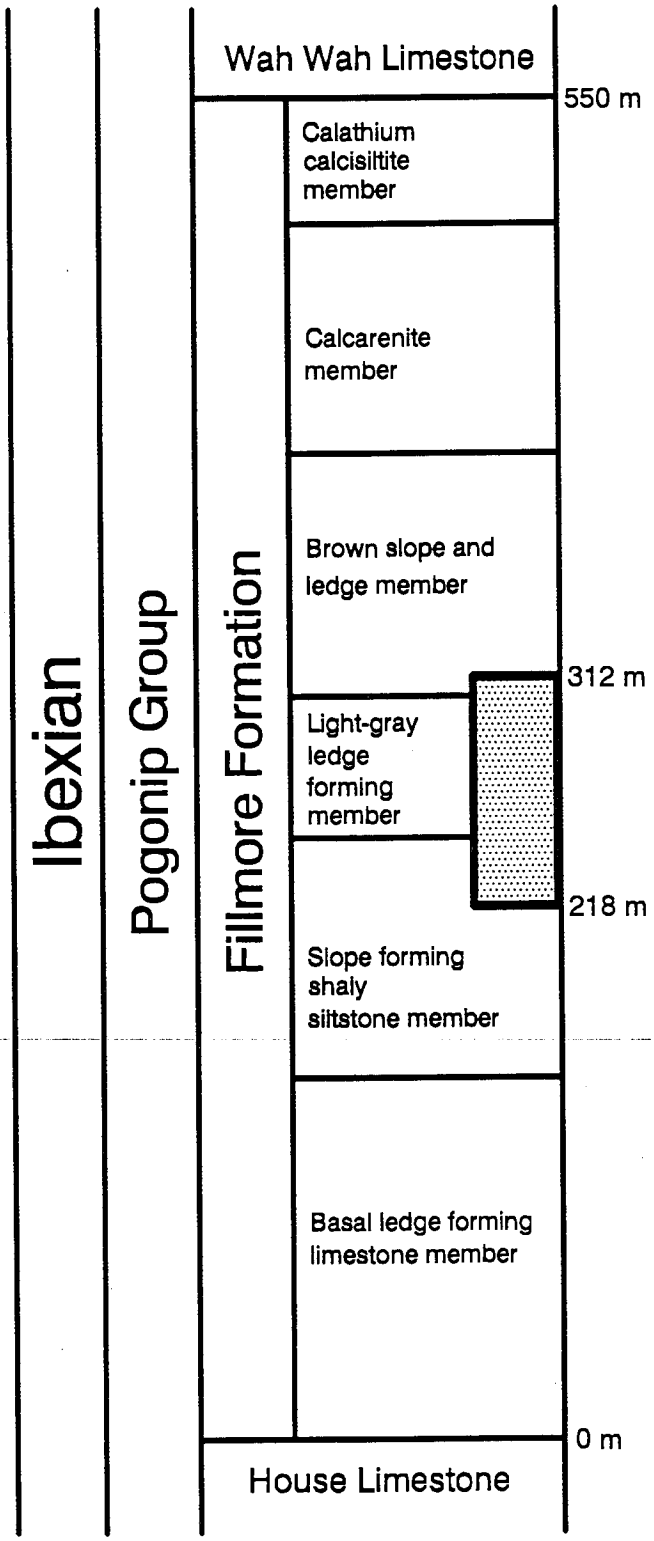

FIGURE 3.—*Stratigraphic column shows location of measured interval in the Fillmore Formation. Informal members of the Fillmore Formation named by Hintze (1951).*

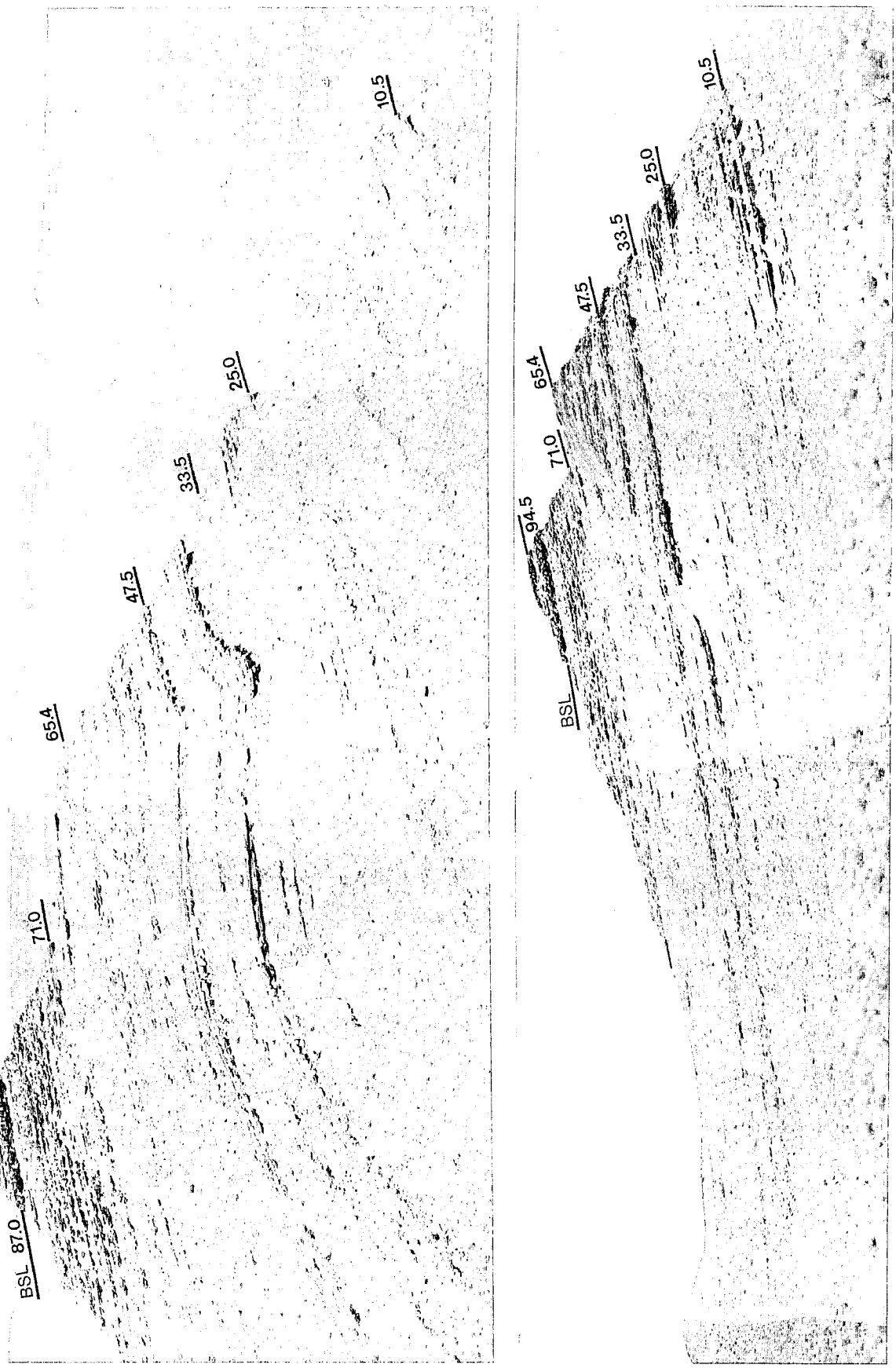

FIGURE 4.—*Two views of section 1: "the pyramid" from the top of section 4, and from the valley to the southeast. Key horizons are labeled in meters. The base of the brown slope and ledge-forming member (BSL) is shown at 87 m.*

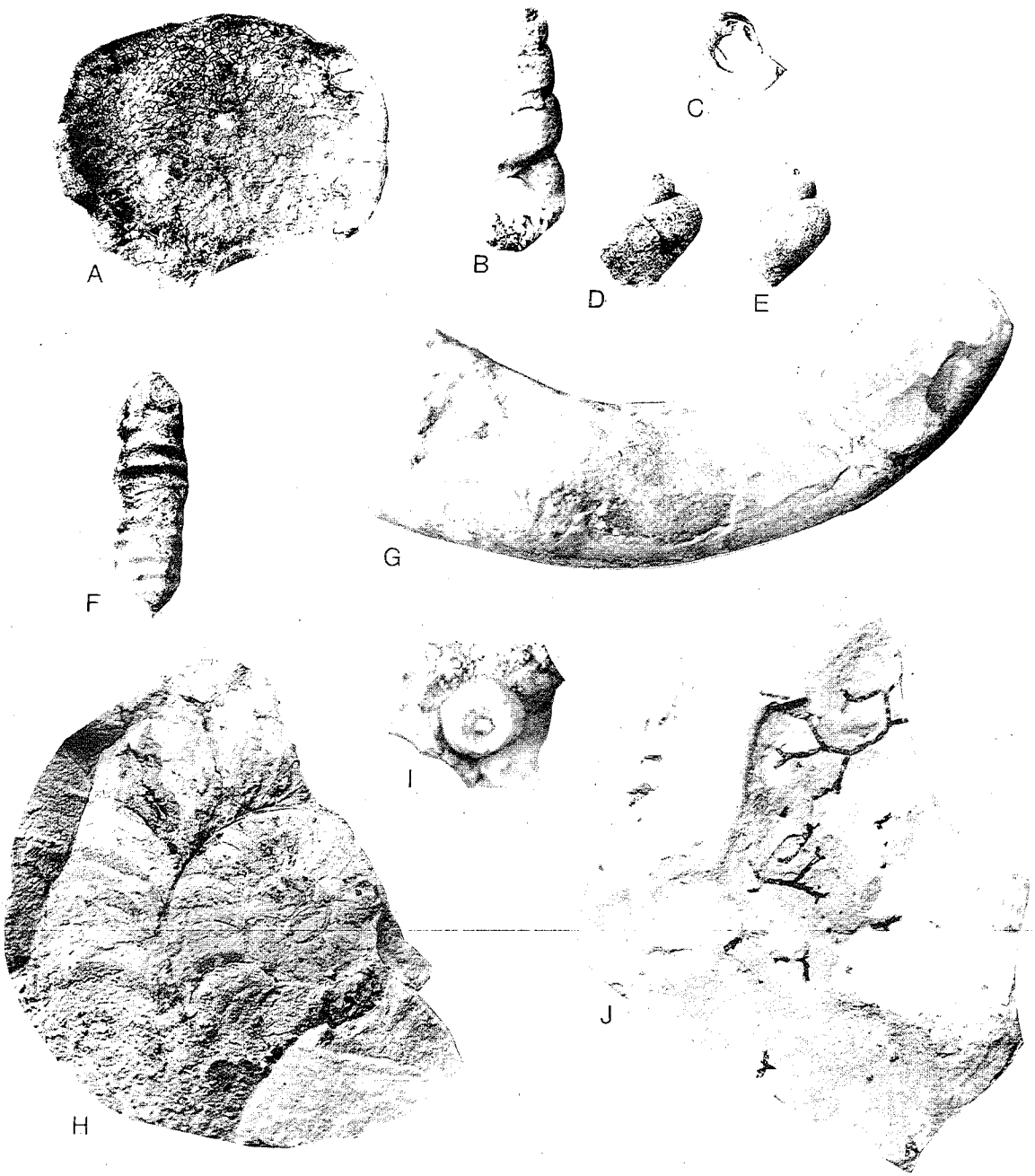

FIGURE 5.—*Some fossils found in the studied sections. All except H and J were blackened with ink and then coated with ammonium chloride. All X1 unless otherwise stated.*

A.—*Lithistid sponge,* Anthaspidella. *X0.5. Section 1 at 19.7 m.*

B.—*High-spired gastropod steinkern cf.* Loxonema. *Section 1 float at 50 m.*

C.—*Gastropod cf.* Macluritella *with some shell preserved. Section 1, 39.9 m.*

D.—*Gastropod steinkern cf.* Seelyia. *Section 1, 90.4 m.*

E.—*Gastropod steinkern cf.* Plethospira. *Section 1, 19.7 m.*

F.—*Orthocone nautiloid living chamber, internal mold. Section 1, 47.8 m.*

G.—*Coiled nautiloid living chamber, internal mold. Section 1, 22.5 m.*

H.—*Coiled nautiloid cf.* Tarphyceras, *internal mold of phragmocone. Section 1, 51.9 m.*

I.—*Echinoderm holdfast. X2. Section 1, 16.7 m.*

J.—Clonograptus *on shale chip shows colonies in various stages of astogeny. X2. Section 1, 47.7 m.*

represented by a few specimens from shale, but is more common on bedding tops of flat-pebble conglomerates. Nautiloids include common annulated orthocones and rarer cyrtocones. While all mollusks are preserved as molds, cephalopods are generally represented by molds of living chambers without phragmocones (figs. 5F, G).

Inarticulate brachiopods are found in particular horizons, generally associated with graptolites where they may be abundant. An articulate brachiopod similar to *Nanorthis multicostata,* which was reported by Jensen (1967) from the Fillmore Formation, occurs rarely in shale.

Mature graptolite colonies collected from shale were primarily *Clonograptus* and *Dictyonema.* They are restricted to certain intervals, such as a horizon at 47.7 m in section 1 that contains a large number of *Clonograptus* in different astogenic stages (fig. 5J) ranging from a few thecae to mature colonies. This size distribution suggests an autochthonous assemblage because different colony sizes were probably not hydraulically equivalent and would have been sorted with transport.

Other lithologies preserve fossils of organisms that probably lived on shaly substrates; this is particularly true of the trilobite packstones discussed below.

Trace fossils. The most common trace fossil in shale units is *Chondrites,* a deposit-feeding trace (Rhoads 1975) (fig. 6). It occurs in almost every shale unit. These burrows are generally 3 to 5 mm across and branch every few cm. The presence of so many deposit-feeding traces suggests accumulation in deep or quiet water (Rhoads 1975).

Small burrows are recognized by contrasts in color between burrow fillings and matrix. One complex burrow type, illustrated in figure 7, is generally 0.5 to 1 cm across and consists of 5- or 6-mm-thick, braided component burrows. These traces were found at 26.2 m, 58.2 m, 63.2 m, and 82.9 m in section 1 and were probably produced by deposit-feeding burrowers.

Coarse burrow fillings with spreite occur at the bottom of calcisiltite-calcarenite beds (fig. 8) and represent fillings of burrows originally made in shale. The burrows are 1 cm or less in diameter. Examples were found at 27.6 m and at 79.4 m in section 1.

Various larger, nondescript burrow casts are found in shale below calcisiltite-calcarenite beds and are vertical or at 45° angles to bedding. These range from a few mm to several cm across.

Two trace fossils were attributed to trilobites. One is a trail found in the float from section 3 at 75.0 m. The other is *Rusophycus,* found at 25.6 m in section 1.

Environmental Interpretation

The diverse fauna, generally evenly distributed bioturbation, and deposit-feeding traces all suggest a quiet, stable environment below fair-weather wave base. Sedimentation was low enough for a range of vagile and some sessile benthos to thrive, but frequent increased sedimentation is indicated by isolated intervals that lack bioturbation and contain well-preserved graptolites or inarticulate brachiopods.

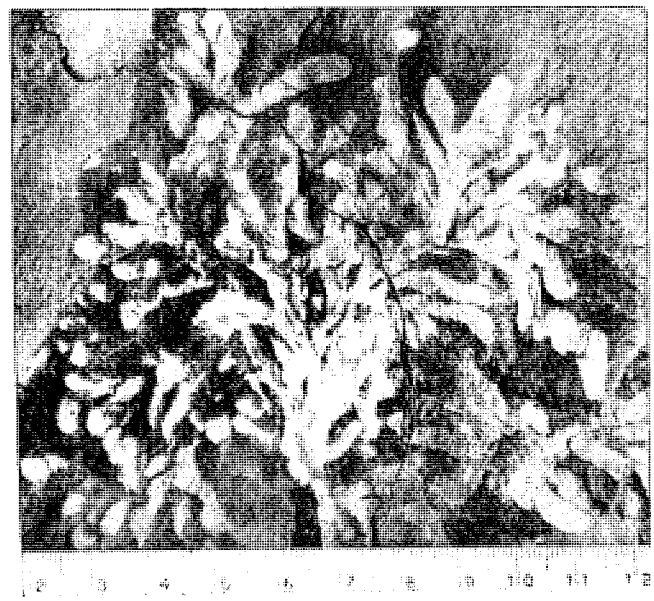

FIGURE 6.—Chondrites *from section 1, 67.1 m.*

TRILOBITE PACKSTONE

Description

Very thin lenses, 1 to 2 cm thick and 30 to 40 cm across, of trilobite packstone occur within thicker shale units in ten horizons throughout the section. These packstones occur more commonly higher in the formation, above the study horizon (Hintze personal communication 1988). They consist predominately of unbroken trilobite plates in a matrix of medium to light gray terrigenous lime mudstone or calcareous shale, which is sometimes pelletal (fig. 9) and is often clotted or granulose (fig. 10). Bases and tops are sharp, but matrix grades into overlying shale.

Trilobite clasts are very large and delicate (figs. 10 and 11) and are normally graded. Where pellets are preserved, shelter porosity, umbrella structure (fines concentrated on upper surfaces of coarse grains), and screening (interstitial fines concentrated in the upper part of unit because they are "screened" from the lower parts by the intervening large grains) are all present, as shown in figure 9. Compaction breakage of fossils (fig. 10) indicates former shelter porosity that was destroyed, along with pellets, during compaction.

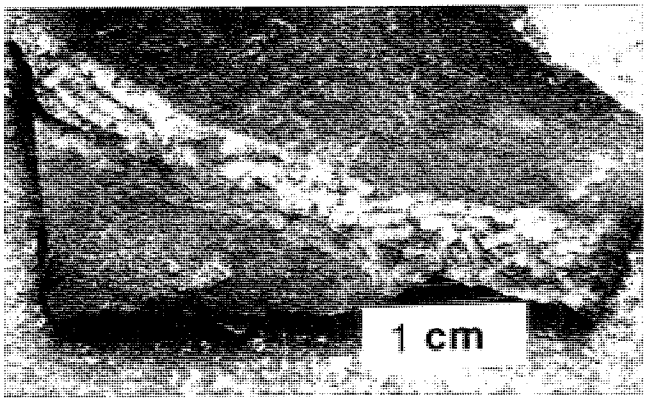

FIGURE 7.—*"Braided" burrows in shale from section 1, 60.0 m.*

Fossils

Trilobites, extracted by acid etching of packstone lenses, include the abundant *Protopliomerella contracta* and *Aulacoparia venta,* and other less common genera such as *Psalikilus, Menoparia,* and a form similar to *Bathyurellus.*

Environmental Interpretation

Very thin beds and laminae of skeletal packstone interbedded with shale, like those described above, are not uncommon elsewhere (Cressman and Noger 1976, Kreisa 1981, and Markello and Read 1981). It is evident from the foregoing description that the Fillmore packstones resulted from isolated reworking or winnowing events that suspended delicate sedimentary particles that later settled without significant breakage. The smallest particles settled later, forming the "infiltration" structures such as shelter porosity, umbrella structures, and screening.

WAVY-LAMINATED LIME MUD

Description

Wavy-laminated lime mudstone and calcisiltite occur as beds within shale units or as thick, terrigenous packages (e.g., fig. 12, upper part). These laminated rocks show very fine-scale interstratification of comminuted shell fragments, sponge spicules, and peloids with clay and silt. Micrite is present, but grains are often larger than characteristic of shale or dense lime mudstone units discussed below. Laminae are graded, but the rocks are fairly well sorted and do not contain many sand-sized or larger fragments. The wavy lamination may result from differential compaction and dissolution of the interstratified water-saturated clay and lime mud or from primary sedimentary structures such as ripples. No definitive ripple marks or other small-scale sedimentary structures were observed, but some wavy-laminated units form mounds 10 to 30 cm across and several cm high.

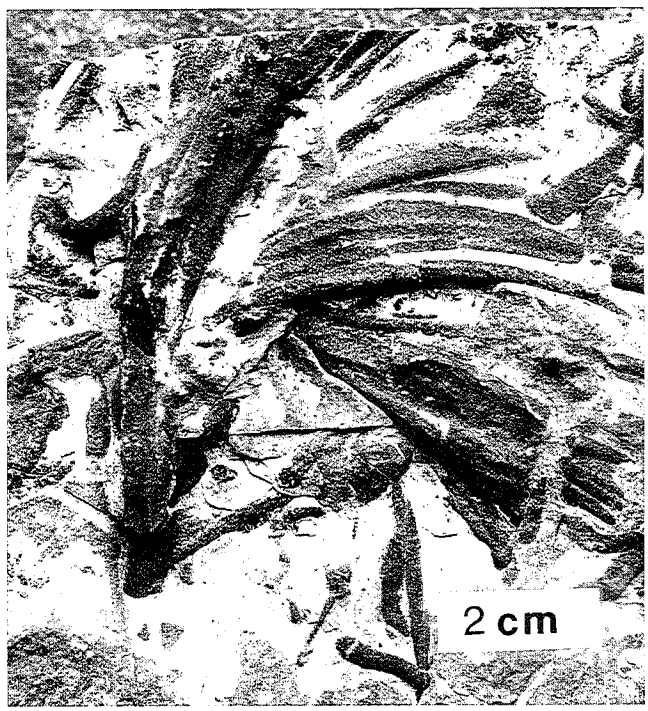

FIGURE 8.—*Spreite burrows on underside of fine calcarenite bed. Section 1, float from approximately 50 m.*

Fossils

Wavy-laminated lime mudstones contain faunal assemblages similar to those of shale, but high-spired gastropods and asaphid trilobites are more abundant, whereas graptolites and nautiloids are diminished. The lack of graptolites may result from taphonomic factors, but gastropods and nautiloids are preserved as they are in shale. The common calcite-replaced siliceous sponge spicules in these rocks may be the remains of sponges that grew locally, or they may have been transported from other environments, but few complete sponges were found. Trace fossils are similar to those of shale.

Environmental Interpretation

The regular alternation between calcareous and terrigenous deposition is a reflection of alternating environmental conditions. Mounds suggest algal binding, because unbound sediments would be gravitationally unstable.

Abundance of silt-sized grains suggests stronger currents than in shale, and the relative restriction of the fauna may result from increased current and higher sedimentation rate or from environmental stresses and fluctuations not directly evident in characteristics of the rocks.

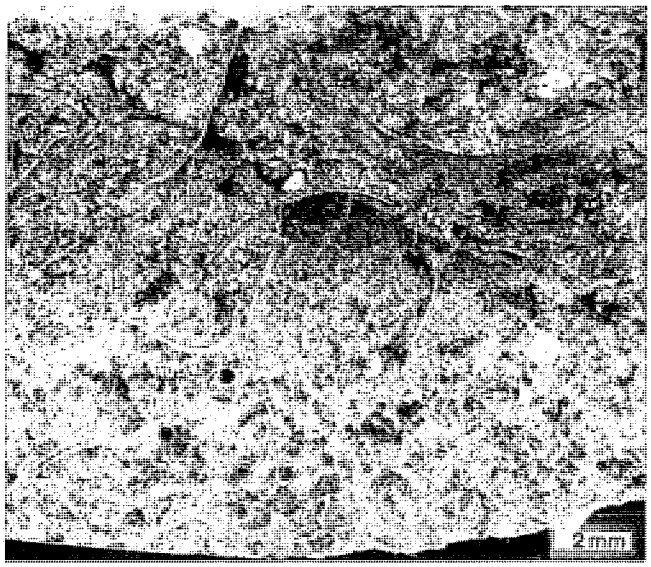

FIGURE 9.—*Projection print from peel of whole-fossil, trilobite pelletal packstone showing large delicate grains and infiltration structures (shelter porosity and umbrella structures). Section 1, 25.5 m.*

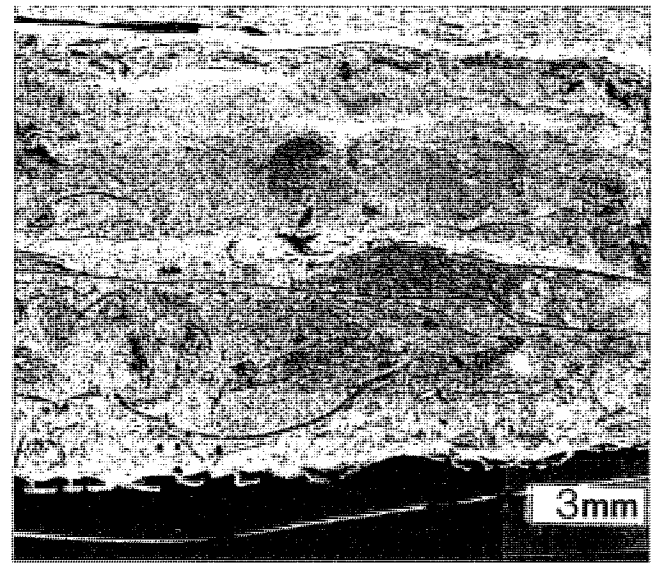

FIGURE 10.—*Projection print from peel of whole-fossil trilobite packstone shows large delicate fossils and compaction breakage that may indicate former shelter voids. Section 1, 31.3 m.*

These characteristics are most likely a result of deposition in shallower water above normal wave base where tides and wave action act to winnow out muds, periodically change sediment type, and where fluctuations in temperature and salinity are common.

DENSE LIME MUD

Description

Relatively unfossiliferous biostromal lime mudstone is exemplified by the unit at 46.0 m in section 1. Such units are generally a few cm to 2 m thick and consist of dense light bluish gray to very light gray lime mudstone.

Dense lime mudstone consists of repeating cycles of three component microfacies (from bottom to top): (1) spiculite; (2) micrite or lime mud; and (3) silt (figs. 13 and 14). These occur in laminae 0.5 to 3 cm thick, which are laterally extensive.

Spiculitic laminae are made of sponge spicule packstone and are lighter in color than lime mudstone, which creates a banded appearance (fig. 13). Largest spicules are approximately 0.4 mm in length and may be monactine or octactine. The volume of spicules varies stratigraphically as well as laterally; calcite-replaced spiculites are better developed in mounds than in biostromes.

Acetate peels document that micrite has an even, massive texture. Grains of dense lime mudstone are generally less than 6 microns in diameter. Silt wisps occur over lime mud laminae (fig. 14) and are differentially compacted.

Blocky calcite occurs in voids (fig. 14), and some burrow fillings consist of light orange dolomite crystals 10 to 20 microns across. These crystals have cloudy cores and clear rims, suggesting formation from growth of scattered penecontemporaneous seed crystals in a fashion outlined by Lee and Friedman (1987).

Dense lime mudstone occurs as extensive, thick beds, such as the 1-m-thick bed at 46.0 m in section 1, or as small mounds, some of which occur in section 1 at 39.4 m, 42.5 m, and 75.5 m (fig. 12). Mounds are generally 20 to 40 cm high and 40 cm to 2 m wide, consisting of well-defined spiculite and lime mud interlaminae. Laminations in these mounds are concave downward toward the bottom, and concave upward toward the top.

No clear evidence of mudcracks was found; however, irregular mm-scale pores and small-scale cracking are present (figs. 14 and 15), suggesting the possibility of desiccation. In addition, collapse structures are highlighted by intrusion of silty laminae into lime mudstone (fig. 15). These structures may be burrows that have been filled from above or fillings of mudcracks. One of the figured structures appears to be a gypsum crystal cast, which is indicative of evaporite dissolution.

Fossils

Dense lime mudstone differs from shale in its more restricted preserved fauna. All but large asaphid trilobites and a few gastropods and sponge fragments are absent. Evidence of burrowing is abundant, and the bioturbation index (Droser and Bottjer 1986) is commonly 3 on a scale of 1 (no bioturbation) to 5 (burrow-mottled structure). Burrows may cover parting planes. They are generally

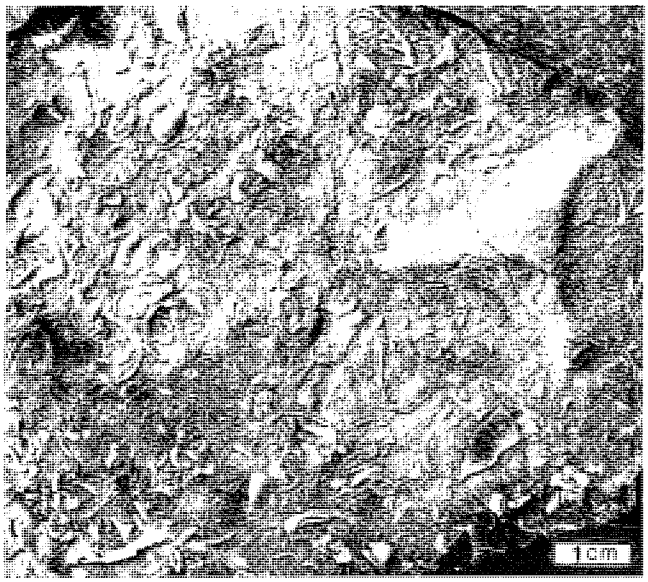

FIGURE 11.—*Top view of hand sample of whole-fossil trilobite packstone shows some breakage but overall preservation of the very delicate fossils. Section 1, 30.2 m.*

preserved in three dimensions and are filled with coarser material such as comminuted platy fragments and peloids. Both horizontal and vertical burrows exist, but vertical burrows are concentrated more in biostromal units.

Environmental Interpretation

The combination of rather deep vertical burrows and large horizontal burrows suggests, not conclusively, a supratidal or intertidal deposition (Cressman and Noger 1976, Hardie and Ginsburg 1977, Laporte 1969) of biostromal lime mudstone, and the restricted fauna, dolomite, and possible evaporite crystal cast help to confirm this interpretation. The spiculite–lime mudstone–silt interbeds are similar to algal tufa-peloidal mud interbeds reported by Hardie and Ginsburg (1977) from a modern inland supratidal marsh. The Fillmore interbeds, by analogy, could have resulted from the alternation of algal mud and storm-deposited spiculite on a supratidal flat. Inside some thicker biostromal units there are frequently very thin beds of small lime mud lithoclasts (fig. 13) that may have formed during storms or by desiccation.

Pratt (1982) concluded that mounds, in general, form in deeper water than biostromes. Coarseness of spiculites in mounds and of grainstone units between lime mud units below mounds, as shown in figure 12, supports a higher energy origin for these mounds in particular.

Dense lime mud frequently overlies wavy-laminated lime mud, especially in mounds. Together with shale these microfacies form a continuum of composition and internal structure and grade into each other vertically. Lime mudstone is commonly directly overlain by a hardground and encrinite with large lime mudstone lithoclasts.

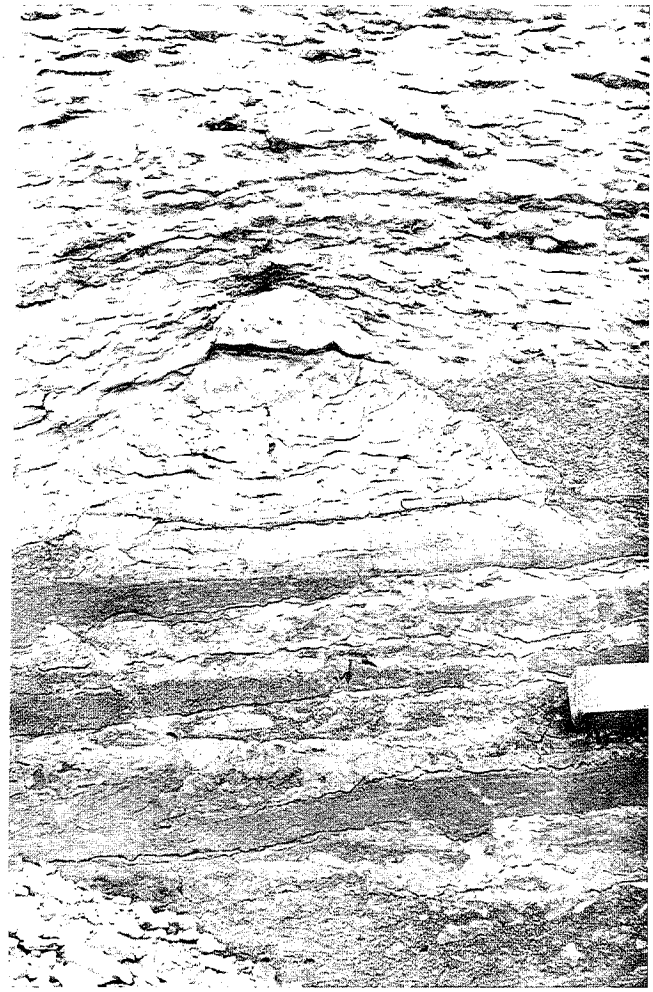

FIGURE 12.—*Outcrop of lime mudstone mound that grew from alternating lime mudstone and calcisiltite-calcarenite beds is covered by wavy-laminated lime mudstone and flanked by encrinite grainstone. Section 1, 68.7 m. Hammer head, lower right-hand corner, for scale.*

REEF MOUNDS

Description

The sponge-*Calathium*-algal patch-reef horizon, which occurs in section 1 at 33.5 m, was studied in detail by Church (1974) and was not examined closely in this study. Only one other studied horizon, a relatively thin unit at 19.6 m in section 1, bears lithologic resemblance to the reef horizon. In this part of the Fillmore, reefs occur at roughly 100-m intervals; there are reef horizons with similar characteristics 100 m below (fig. 1, dual roadcuts and northeast corner of "study area") and 100 m above (northern part of western border of study area) this horizon.

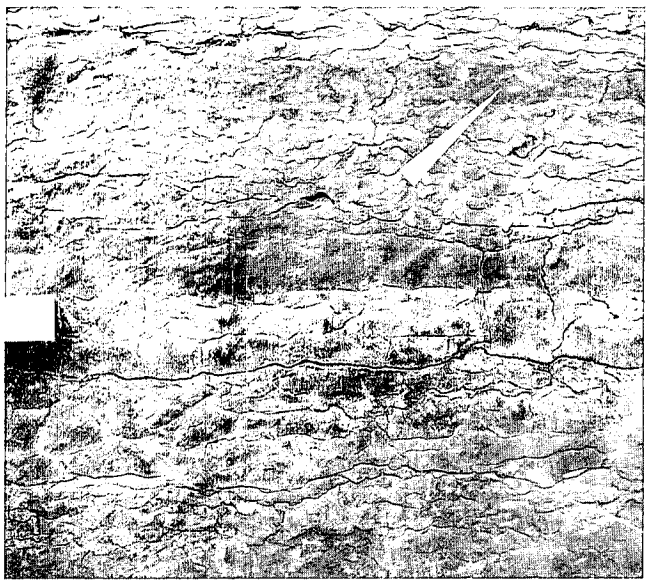

FIGURE 13.—*Outcrop of dense lime mudstone unit showing banded appearance that results from interbedded micrite and spiculitic calcisiltite. A thin, dark band of lithoclastic grainstone occurs in the upper right-hand corner of the photograph (arrow). Outcrop photograph. Section 2, 26.3 m.*

Figure 16 shows typical reef lithology from section 1 at 19.6 m in which echinoderm grains outline a digitate, clotted micrite framework suggestive of thrombolite growth as described by other workers (Aitken 1967, Kennard and James 1986, Pratt and James 1982).

Church (1974) provided information regarding gross form of the reefs. They are elongate, loaf-shaped bodies 1 to 1.5 m high, 2 to 3 m wide, and 30 m long. They rise 1 m above contemporaneous rocks and are spaced approximately 10 m apart. This agrees with observations of other thrombolite occurrences by Aitken (1967).

Fossils

Reef lime mudstones contain very diverse assemblages, including the alga *Calathium*, sponges *Archeoschyphia* and *Anthaspidella*, a variety of echinoderms, asaphid and pliomerid trilobites, and orthocone and coiled nautiloids. Church (1974) described this assemblage more fully. The chief distinction between this and shale communities is the dominance of filter-feeding encrusting organisms, such as sponges and echinoderms. Figure 5H shows how cephalopod preservation is more detailed and includes phragmocone in reef lithologies. The shale assemblages are compatible with turbid environments, whereas the reef assemblages were adapted to clear water.

Environmental Interpretation

The abundant stenotypic fauna indicates that reefs were deposited subtidally rather than intertidally like lime mudstone units discussed above; to cover these reefs, water would have been at least 1 m deep over the surrounding sea floor. Pratt and James (1986) concluded that thrombolite mounds grew in agitated shoal waters of the subtidal zone and that more complex mounds indicate more open water. Reefs probably formed because of a reduction in terrigenous sedimentation or, as indicated by Church (1974), an increase in agitation.

FIGURE 14.—*Projection print of peel of laminated lime mudstone showing progression from silt (A) through spiculite (B) and lime mudstone (C). Section 1, 38.9 m.*

CALCISILTITE AND CALCARENITE

Description

Calcisiltite and calcarenite units range from medium gray to medium dark gray and weather dark olive gray. They are generally very fine grained, thin bedded, and internally thinly laminated. They occur interbedded with shale or wavy-laminated lime mudstone.

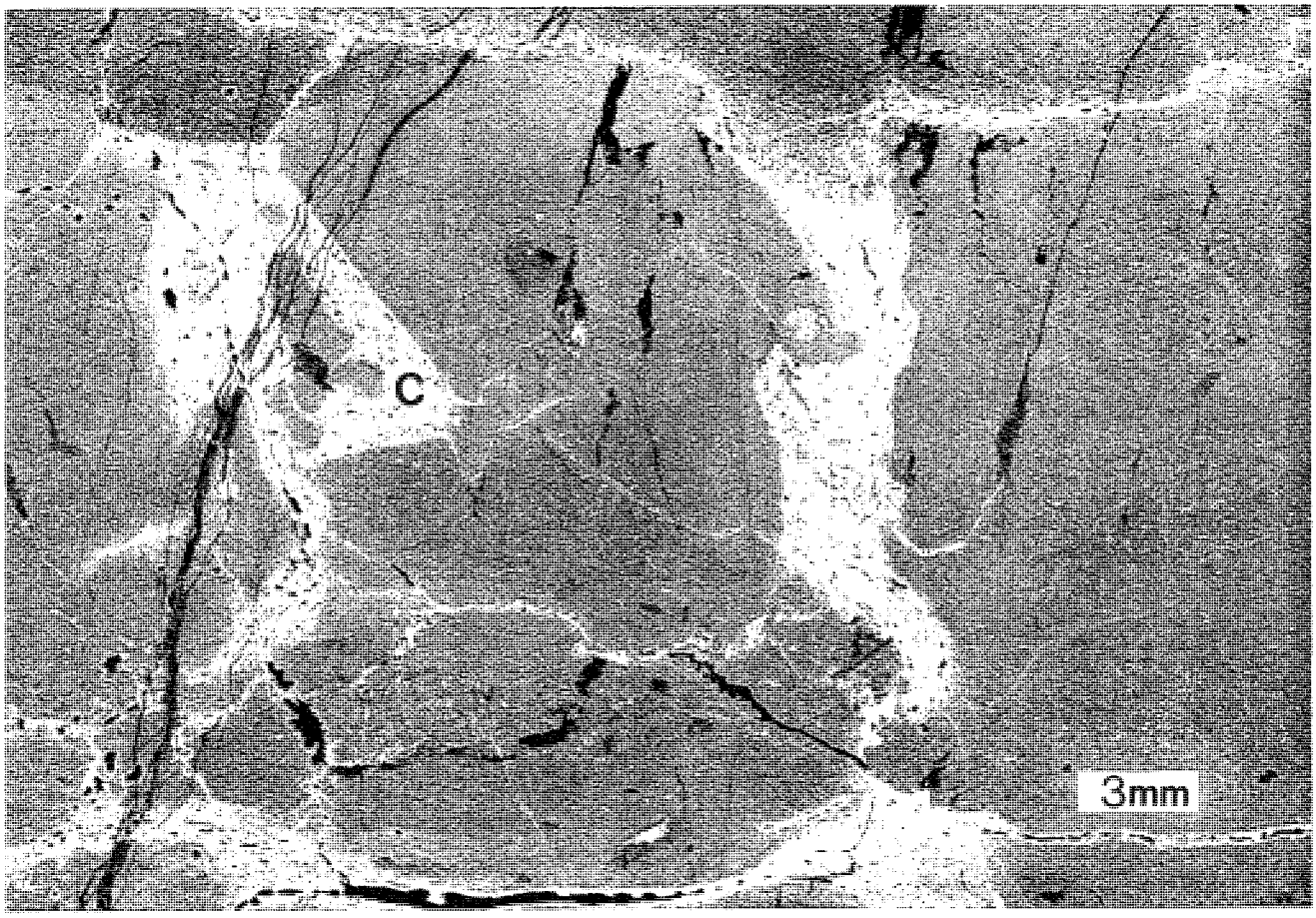

FIGURE 15.—*Projection print from peel of lime mudstone unit shows collapse structures. Form on the left (C) resembles a crystal and may represent lost evaporites. Section 1, 38.9 m.*

Coarser calcarenite grains are mostly trilobite fragments with some echinoderm ossicles. Trilobite fragments are comminuted (fig. 17), but retain a platy character, being twice as long as more equant echinoderm grains. Medium- to fine-sand-sized grains in calcarenites are usually not identifiable taxonomically. Lime mud matrix and terrigenous silt and clay are important constituents in finer-grained units and are more abundant in the top 0.5 to 1 cm of beds.

Calcisiltite-calcarenite grains range from very coarse sand through silt sizes and are mostly medium-sand to silt-sized and moderately well sorted. Commonly only the top 0.5 to 1 cm of a bed is graded, and grain size ranges generally through less than 1 Phi division. However, in some cases grading is abrupt and dramatic. Goldring and Bridges (1973) indicated that this type of grading can be caused by slow deceleration of suspension currents.

Most calcisiltite-calcarenite beds are planar or hummocky laminated; some have ripple cross-lamination. Very fine cross-laminated ripples occur rarely. Wavelengths are 10 cm, and heights from trough to crest are 1 to 2 cm. A few units show 10–15-cm-thick cross-bed sets.

Laminations range from 2 to 6 mm thick and may thin to about half thickness in the upper 1 cm of the bed. Each lamina is internally graded and more terrigenous and silty toward the top. These silty laminations can be observed on peels made from deeply etched slabs.

Authigenic silica is an important part of many insoluble residues. It replaces trilobite fragments, occurs interstitially, and commonly follows terrigenous parts of laminae.

Chert, illustrated in figure 18, is light bluish gray with 0.5-mm reddish brown flecks and occurs as elongate nodules that follow cracks or burrows. Chertification does not disturb primary laminations, but nodules are typically twice as thick as host beds, which shows that they formed early, before compaction. Chert is limited to calcisiltite-calcarenite, which suggests either enhanced susceptibility or frequent exposure to chertifying conditions.

Silica may have come from abundant sponge spicules, as observed elsewhere by Lee and Friedman (1987), or from surrounding shale, but the mechanism of chertification was not determined. Because chertification pre-

FIGURE 16.—*Projection print from peel of "reef" lime mudstone showing large* Calathium *(C) and echinoderm ossicles in lime mud matrix. Pattern formed by echinoderm ossicles outlines possible digitate thrombolite structure. Section 1 at 19.6 m.*

ceded compaction, it probably did not result from postburial mechanisms, such as groundwater mixing as suggested by Knouth (1979).

Cement consists of overgrowths on echinoderm grains and blocky calcite filling. Dolomite rhombs sometimes occur in spaces between trilobite grains (fig. 17) and may have formed by association with clay minerals in surrounding shale, as explained by Kahle (1965).

Beds range from 0.5 cm to 20 cm thick, but most are between 3 and 5 cm thick; they rarely exceed 10-cm

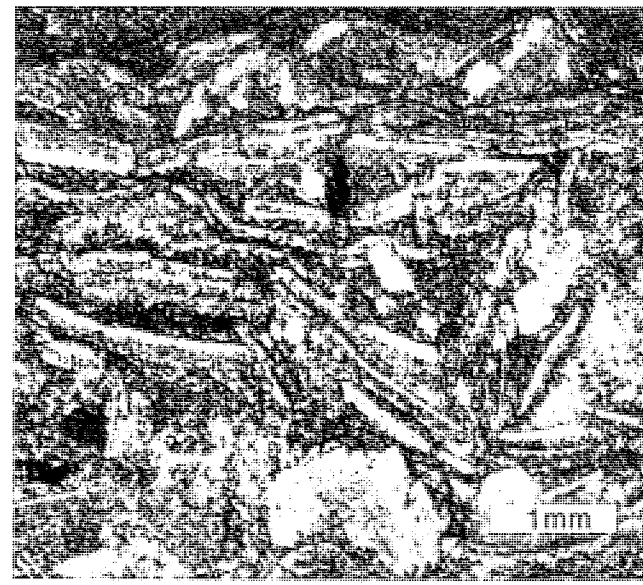

FIGURE 17.—*Projection print of peel of very coarse calcarenite showing comminuted, silicified, trilobite fragments and interstitial dolomite. Section 1, 26.2 m.*

thickness. Bases of calcisiltite-calcarenite beds are generally sharp and planar, indicating sudden onset of deposition. Casts of a variety of exhumed trails suggest some predepositional erosion. Bedding tops are generally sharp, but some are gradational with overlying shale. Frequently there is evidence of discontinuity at the top, such as brown staining and concentrated bioturbation.

Calcisiltite-calcarenite beds are frequently locally discontinuous and appear as starved ripples or to fill depressions (fig. 19), and lenses are 15 cm thick and 1 to 3 m wide. Thinning is associated with bottom irregularity, and some beds are discontinuous, forming flat-topped hemispherical nodules and gutter casts 10 cm thick. Finer-grained lenses are commonly 1 to 2 cm thick and a few tens of cm wide. Thicker calcisiltite-calcarenite beds are traceable over wide areas despite local variation, and some units appear in all measured sections as calcisiltite-calcarenites or laterally equivalent flat-pebble conglomerates.

Vertical irregular stylolites are common and outline polygons 5 to 15 cm across on both upper and lower surfaces of calcisiltite-calcarenite beds (fig. 20). Rarely, parts of these layers are curled upward like mudcracks, but a single piece of curled calcisiltite-calcarenite may be 50 or more cm across and include several polygons, as is the case with the specimen in figure 20. Curvature of individual polygons does not occur in situ nor among pebbles in flat-pebble conglomerates. The observed curvature is likely to have been caused by differential compaction around underlying irregularities, as shown in figure 19.

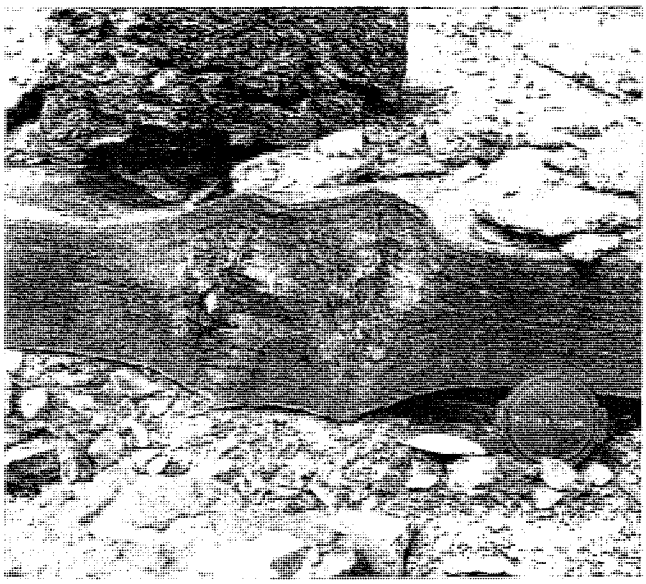

FIGURE 18.—*Outcrop of chert nodules in very fine calcarenite shows differential compaction around nodules and even planar-lamination that continues through nodules. Section 5, 49.0 m. Camera lens cap for scale.*

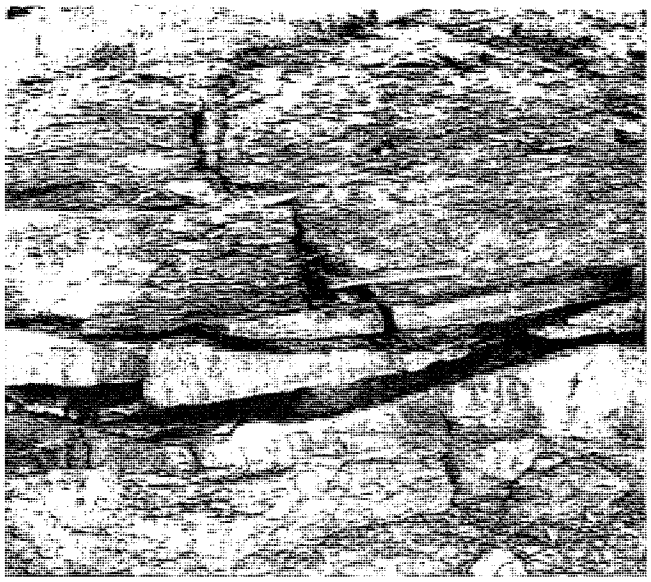

FIGURE 19.—*Outcrop of fine calcarenite lens, the thickness and shape of which is apparently controlled by underlying topography and differential compaction. Hammer lies directly on calcarenite bed that is underlain by two megarippled flat-pebble conglomerate beds. Section 1, 71.0 m.*

Four characteristics suggest that these are syneresis cracks: they (1) lack V-shaped cross sections typical of mudcracks; (2) they form irregular polygons; (3) they occur in medium-sand calcarenite units; and (4) they occur in units that have characteristics suggesting a subtidal origin. Possibly cracks did not originate in calcarenite but in underlying shales, and were later closed and stylolitized as both shales and calcarenites were compacted.

Fossils

Body fossils are limited to thin veneers on lower surfaces of calcisiltite-calcarenite units and were presumably exhumed directly from the underlying shale. Like the shale, these faunas are dominated by trilobites.

Bioturbation is most commonly concentrated in the upper few cm of most beds (fig. 21) or is represented by escape burrows. Both are characteristic of sudden deposition (Goldring and Bridges 1973).

Environmental Interpretation

From the patterns of bioturbation it is clear that these units were formed during relatively short-term events, perhaps storms. The lack of whole-body fossils within beds is an indication of both short duration (preventing colonization within a bed) and moderately strong currents, which could transport silt and sand but not suspend very coarse fossils.

FLAT-PEBBLE CONGLOMERATE

Description

General features. Fillmore flat-pebble conglomerates vary texturally. They occur in a single matrix-composition gradient with terrigenous lime mud (fig. 22E, F) at one extreme and very coarse echinoderm arenite, or "encrinite" (fig. 22A), at the other. Intermediate textures are calcisiltite packstones, fine calcarenite packstones (fig. 22D), medium-sand-sized trilobite packstones and grainstones (fig. 22C), and coarse-sand-sized trilobite-echinoderm grainstones (fig. 22B). All of these lithologies are also found in the section without lithoclasts, and there are a few examples of each where a flat-pebble conglomerate can be traced laterally into a non-lithoclastic unit. The following discussion refers to three categories of flat-pebble conglomerate based on matrix texture and includes (1) lime mud matrix (less than 10% grains); (2) trilobite-dominated matrix (less than 75% echinoderm material); and (3) encrinite matrix.

Encrinite-dominated conglomerates differ from other units in several important ways. They are matrix supported and lack infiltration structures such as shelter voids, umbrella structures, and screening, which are found in other flat-pebble conglomerates. Amalgamation (the stacking of event deposits within a single bed) occurs only in encrinite- and coarse trilobite grainstone-dominated units.

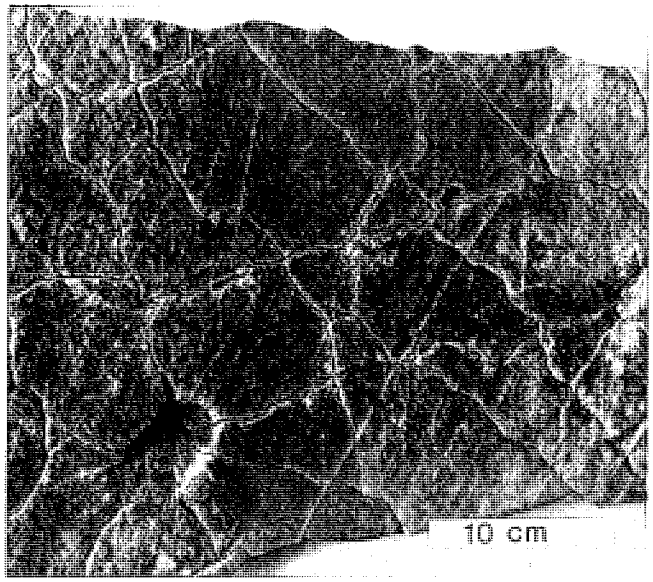

FIGURE 20.—*Syneresis cracks on upper surface of a typical fine calcarenite. Note irregularity of polygons and stylolitization along cracks. Straight lines are probably tectonic in origin and can be found in all lithologies. Origin of pits is not known. Section 1, 16.9 m.*

FIGURE 21.—*Top view of loose slab of calcarenite shows bioturbation concentrated on upper surface. Scale in cm. Section 1, 16.9 m.*

Beds with encrinite matrix commonly overlie lime mudstone and iron-stained silicified surfaces. Trilobite-dominated units occur in more shaly parts of the section and are frequently associated with calcisiltite-calcarenite beds and wavy-laminated lime mudstone. Units with pure lime mudstone matrix occur in association with lime mudstone or shale.

Cementation of matrix in Fillmore rocks was commonly submarine. Encrinite matrix has a mosaic of poikilotopic syntaxial rim cement surrounding echinoderm grains. Though compaction structures, including sutured grain contacts (figs. 22C and D) and fossil-pierced lithoclasts, are common, they do not occur between echinoderm grains, suggesting early cementation. Lime mud laminae within or on top of open encrinite, without infiltration, may also indicate early cementation.

In trilobite- or mud-dominated matrix, blocky cement is present around trilobite clasts, in addition to syntaxial rim cement on echinoderm clasts. Such rocks may have been cemented early, and some are truncated by ripple-like surfaces that cut pebbles and matrix alike.

Dolomite is a minor component of flat-pebble conglomerates. Larger percentages occur in only a few muddy trilobite-dominated packstones. Dolomite is patchy and commonly occupies shelter voids. Texture varies from isolated rhombs to a xenotrophic fabric.

Lithoclasts. Lithoclasts are similar to (and apparently derived from) in situ beds in the sections. They include pure and silty laminated lime mudstone (figs. 22E and F), calcisiltites to fine calcarenites (figs. 22B, C, and D), coarser calcarenites (fig. 22B), whole fossil wackestones, and pieces of other flat-pebble conglomerate beds (fig. 22B) ("multigeneration" clasts of Markello and Read 1981). Most lithoclasts are fine calcarenite to siltite or lime mudstone, as is true of many other formations (Berry 1962; Markello and Read 1981, 1982; Sepkoski 1982).

Pebble size, shape, and orientation are related to transport distance and energy along with durability of clast material. A wide spectrum of lithoclast characteristics is present in the Fillmore. Lithoclasts are generally 2 to 5 cm across, though some as large as 40 cm across and others as small as coarse sand were noted in the sections. Pebbles that overlie possible source beds are commonly 5 cm or more in diameter, whereas those that do not are usually only a few cm across.

Pebbles in flat-pebble conglomerates are usually poorly sorted, as shown in figure 22C. Pebbles in the few well-sorted units (fig. 22E) are also well rounded, small, and not associated with possible source rocks, suggesting that sorting is also related to transport. More than 90% of flat-pebble beds are not graded. Normal grading is present in a few beds.

About 80% of pebbles are well rounded, but where obviously derived directly from underlying beds they are angular.

Lithoclasts are usually oriented either horizontally within beds (fig. 22B) or are imbricated at 10° to 30° (fig. 22C). Some thicker beds contain flat pebbles that are oriented nearly vertically, or "edgewise"; these are generally jumbled, without any preferred azimuthal orienta-

tion or consistent inclination. Based on flume experiments, Futterer (1982) concluded that consistent imbrication results from current action, and jumbled edgewise accumulations are produced by waves.

Calcisiltite-calcarenite clasts are typically tabular, whereas lime mudstone clasts are more frequently subspherical or irregular in shape. They are little compacted and preserve internal laminations, burrows, and fossils. Thus, calcisiltites and fine calcarenite intraclasts were probably well lithified before deposition and are usually large. Lime mudstones were less lithified, and when lime mud occurs in a heterogeneous lithoclast, it forms eroded reentrants. Other lithologies, such as coarse calcarenites and encrinites, were either not frequently lithified early or were not easily disrupted to form clasts.

Evidence of intraclast deformation is lacking. Radial, spar-filled cracks 0.5 mm wide are common in lime mud intraclasts (see figs. 22E, F). The cracks do not continue in surrounding matrix. Rather than indicating syndepositional deformation, these cracks may have formed as a result of syneresis or as matrix was compacted around relatively brittle pebbles.

Burrows occur in pebbles but do not enter surrounding matrix. Burrows preserved in surrounding matrix on surfaces of lithoclasts show that clasts were hard enough to resist burrowing.

Lime mudstone clasts with siliceous iron-stained rinds are conspicuous in encrinite matrix and are frequently associated with similarly stained underlying hardgrounds. Such alteration indicates that pebbles were exposed for long periods and supports the conclusion that encrinite intraclast beds represent reworked lags, rather than single-event deposits.

The fine-grained character of most lithoclasts may be associated with the earlier cementation of calcisiltite-calcarenites relative to conglomerates. Intraclast composition in encrinite matrix suggests that lime mudstone clasts were softer than calcisiltite-calcarenite clasts. Encrinite conglomerate beds contain predominantly lime mudstone clasts, but there are more beds that contain approximately 25% lime mudstone clasts than those that contain 75%. Apparently, lime mudstone lithoclasts were destroyed more easily in transport than were clasts of coarser-textured lithology and, thus, occur most often when derived locally or as remnants among more durable calcisiltite grains.

Bedforms. Flat-pebble conglomerate beds have sharp bases. Generally these bases are smooth, but some are wavy to irregular with wavelengths of 5 cm or so; irregular surfaces are probably load casts. Gutter casts are common and range from 3 to 20 cm across. They may occur on bottoms of beds or as isolated fillings. Lime-mud mounds commonly control bottom shape, and there are occasional channel-like forms, especially below beds with encrinite matrix.

Upper surfaces of many flat-pebble units have ripples with wavelengths of 1.5 to 3 m and heights of 10 cm or so. Some ripple beds (fig. 23) are locally discontinuous, suggesting sediment-starved conditions. Internal imbrication patterns of intraclasts suggest current directions normal to ripple orientations.

Flat-pebble conglomerate beds average between 5 and 20 cm thick, but range from 1 to 40 cm thick. They are locally variable, commonly with lateral shifts in lithoclast composition or loss of lithoclasts altogether. Thicknesses also change dramatically. Most beds may be traced over several hundred meters. Such variations are apparently a common phenomenon of storm beds, for such patterns have also been reported in storm-dominated units elsewhere by Kreisa (1981), Sepkoski (1982), and Whisonant (1987). Kreisa (1981) suggested that similar variability in shell beds results from patchiness of benthic communities and lack of lateral transport. This explanation also applies to flat pebbles, where lithification and exposure might also be patchy. Alternatively, bottom topography could control thickness.

Fossils

Fossils are not generally well preserved within flat-pebble conglomerates, and it is difficult to determine which organisms actually lived in association with the pebbly bottom. For example, the gastropod *Macluritella* (fig. 5C) may have lived on the tops of flat-pebble units where it is most commonly preserved, or it may have been reworked from shale. Many fossils were obviously reworked and retain mud in small pores and folds. Others (e.g., rare articulated trilobites on bed tops) were either killed and suspended during the flat-pebble event or smothered subsequently. Despite these ambiguities, echinoderm holdfasts on intraclasts (Thomas E. Guensburg personal communication 1991) and burrows made in the matrix under pebbles demonstrate that the pebbly sediment was populated in at least a few cases.

Environmental Interpretation

These combined characteristics suggest that units with trilobite-dominated matrix were produced by single turbulent events, whereas encrinites were probably formed by reworking or "condensation." Such reworking destroyed weaker bioclasts, left an echinoderm lag, and destroyed all but the most durable or latest-formed lithoclasts and infiltration structures. These units are interpreted as storm deposits and, as such, will be explained more fully in conjunction with the storm-depositional model below.

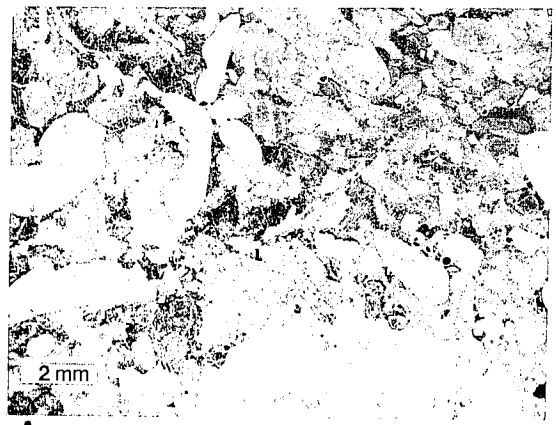

A

B

C

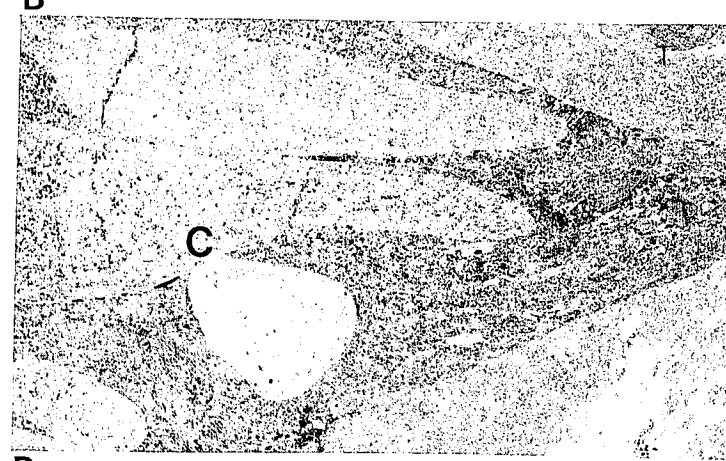

D

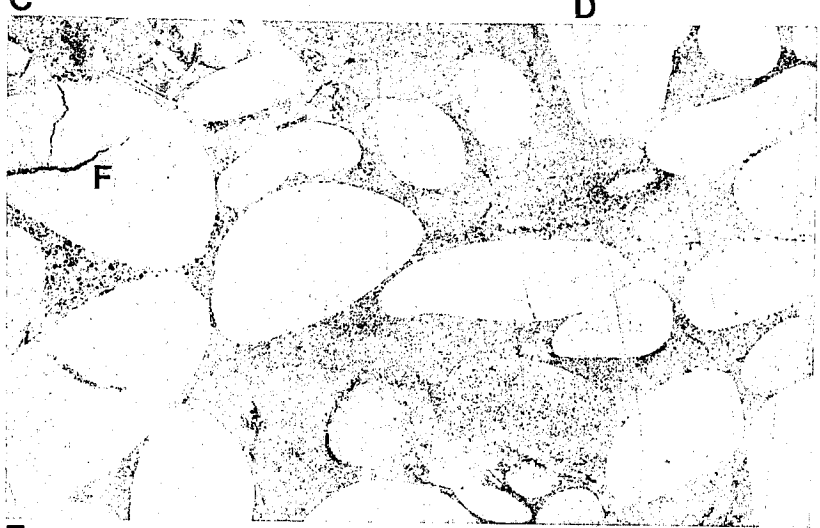

E

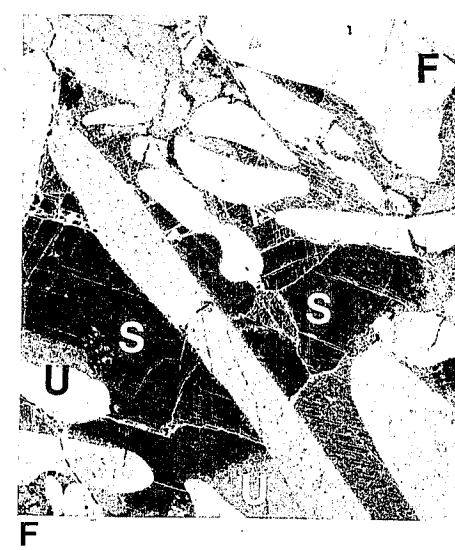

F

HARDGROUNDS

Description

Section 1 contains many examples of hardgrounds or firmgrounds. All share certain characteristics, most falling into a few recurrent types, but a few are distinct enough to use as keys for lateral correlation. Common characteristics, as well as the most abundant types of surfaces, are discussed below.

Hardground characteristics. Substrate type, amount of ferruginous stain, encrusting or boring organisms, and degree of truncation are the most distinguishing characteristics of hardgrounds.

Iron-stained silicified rinds are readily apparent evidences of discontinuity surfaces. Moderate reddish brown alteration does not appear until a surface has been exposed to recent weathering, but stain is a compositional characteristic of a discontinuity surface and not purely a Recent weathering phenomenon because such stains have only developed on certain bedding surfaces. Rinds are as thick as 1 cm, but most are less than 1 mm, and some hardgrounds lack any apparent stain. On a given surface, the rind is thicker in topographically higher areas, but the weathering factor makes it difficult to assess the significance of this.

Other workers have reported surficial mineralogical alterations as evidence of hardground formation (Koch and Strimple 1968, Lindstrom 1963, Shinn and others 1969). The stain probably results from oxidation of pyrite into limonite. Church (1974) attributed the silicification of the reef horizon to contact with overlying shale. However, this does not explain silicified rinds that are not in direct contact with shale. Wilson (1975) interpreted such crusts as evidence of early contact with meteoric water. Clearly, silicification postdated firmground burrowing activity; most burrows are themselves surrounded by rinds. If the rinds were formed simply by meteoric contact, then it must be hypothesized that the majority of hardgrounds were first partially lithified, burrowed, then exposed to meteoric water, silicified, and then finally covered with encrinite. The most likely mechanism is that the rinds formed diagenetically on substrates that had been altered by exposure at the sediment-water interface. Such alterations might include coatings and impregnation by organic matter and biotic micritization.

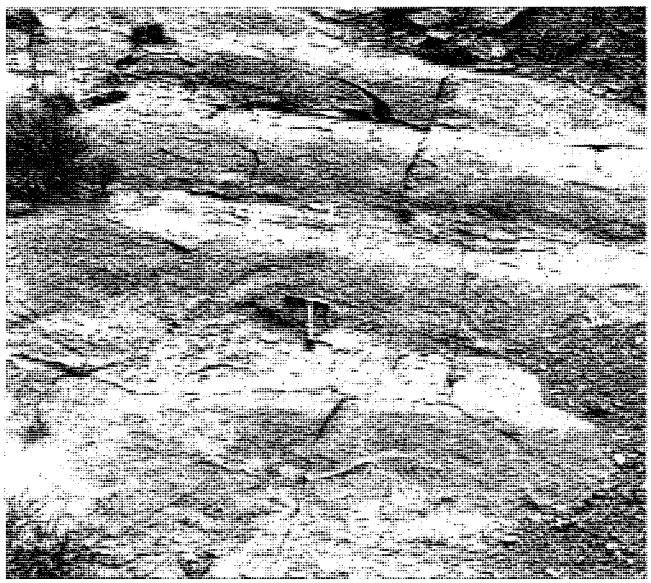

FIGURE 23.—*Large ripple marks exposed on bedding plane. Outcrop in gully between sections 4 and 5. Approximately at the 20-m level of section 1. Note hammer, near center, for scale.*

Hardground categories. Common hardground and possible hardground types in the Fillmore Formation contain the above characteristics to varying degrees. These types are (1) stained flat-pebble conglomerates; (2) ripple-carved flat-pebble conglomerates; (3) truncated calcisiltite; (4) lime mudstone surfaces; (5) lime mudstone mounds; and (6) surfaces of large reefs.

FIGURE 22.—*Flat-pebble conglomerates showing different matrix and pebble compositions. Projection prints of acetate peels, all X5. B = in situ bed, C = sutured contact, H = hardground, M = mudstone, P = pebble(s) or lithoclasts, S = shelter porosity, and U = umbrella structure. All from section 1.*

A.—*Encrinite matrix. Note lack of lithoclast support. 29.7 m.*

B.—*Trilobite matrix with 50% echinoderm grains. Note shelter voids (S), multigeneration clasts showing greater erosion of lime mud or clay (M), and remnants of trails (T) on lithoclasts. 29.4 m.*

C.—*Trilobite-dominated matrix showing poorly sorted, mixed lithoclasts and sutured grain contacts (C). 77.9 m.*

D.—*Fine trilobite packstone matrix with homogeneous, well-rounded, well-sorted calcisiltite and calcarenite pebbles. 63.4 m.*

E.—*Lime mudstone matrix and well-sorted, well-rounded lime mudstone clasts. Note fracture (F) in pebble. 2.3 m.*

F.—*Lime mudstone matrix showing extensive shelter porosity (S) and umbrella structure (U). 44.5 m.*

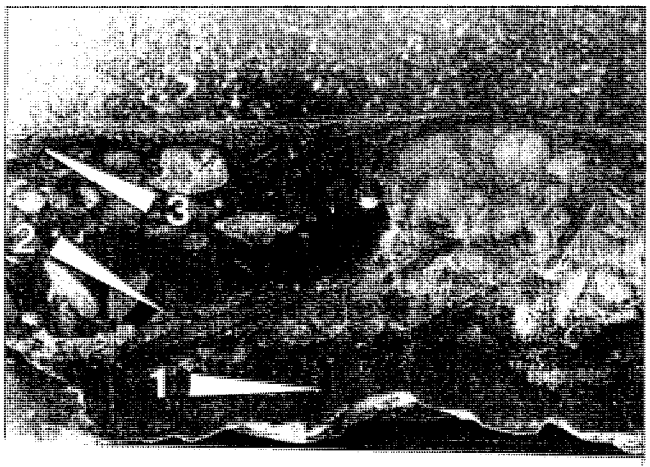

FIGURE 24.—*Etched slab shows ripple-form truncation surface (3) developed on a flat-pebble conglomerate. Note how pebbles are truncated with matrix. Two other discontinuity surfaces (1, 2) occur in this sample. Section 1, 19.0 m. Scale in mm.*

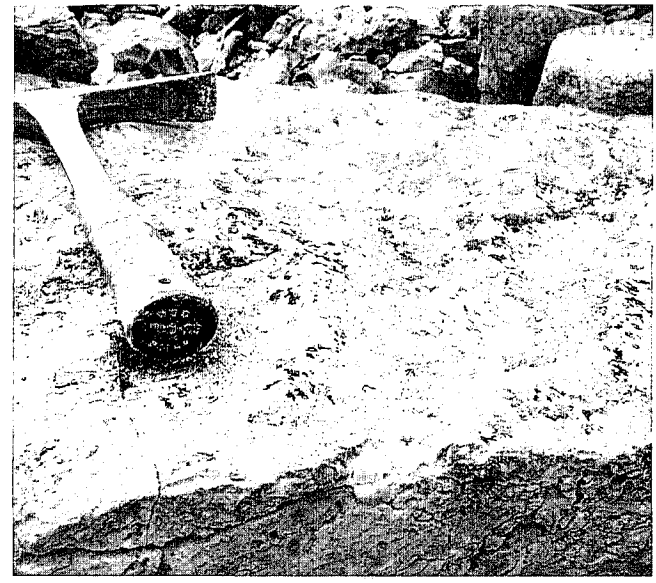

FIGURE 25.—*Bedding plane view of ripple-form truncation surface, which shows similarity to "normal" oscillation ripples. Float from section 2 at 24.1 m.*

The most common possible hardgrounds are flat-pebble conglomerates with iron-stained pebbles that protrude from their surfaces. Clearly the intraclasts were lithified, but without proof of matrix lithification, it may be more appropriate to call these "pavements."

Ripple-carved flat-pebble conglomerates (figs. 24 and 25) are common in the lower Fillmore Formation. These eroded surfaces are most often cut across medium to coarse trilobite-dominated matrix and pebbles of various compositions. More rarely the same morphology will occur on other rock types, such as reef lime mudstone.

Figure 24 shows how pebbles were eroded to exactly the same level as matrix. Ripples are usually sharp crested and have approximately 10-cm wavelengths and amplitudes of 1 or 2 cm. Some surfaces show interference ripple patterns, but most have linear crests.

An acetate peel from the specimen in figure 24 shows that silicification is limited to truncated pebbles. Such a pebble is entirely silicified whereas adjacent pebbles just under the surface are untouched.

Such surfaces were observed by Osmond (1963) in rocks in the Garden City Formation. He attributed this phenomenon to abrasive action of flowing silt-laden water and believed that both pebbles and matrix were lithified when cut. At this time there is no suitable explanation for the formation of ripple marks by erosive or corrosive mechanisms.

A few very fine calcarenite and calcisiltite units have truncated upper surfaces. These surfaces are only lightly stained and have a morphology dominated by low-relief undercut mushroomlike shapes, which indicate that the surface was at least firm.

Hardgrounds on lime mudstone units are generally iron-stained and commonly covered by coarse encrinites (fig. 26). Relief on lime mud hardgrounds ranges up to 15 cm; various degrees of irregular truncation relief are shown in figures 27 to 30. Such surfaces are frequently dominated by mushroomlike forms. These surfaces are commonly perforated by numerous meandering tubes 2 to 4 mm in diameter (fig. 31). They cut longitudinally parallel to the surface and show that lime mudstone hardgrounds are also truncated or erosional in nature. Complex canal systems probably originated as networks of living chambers just under the surface with more or less perpendicular access canals to the surface, as reported by Lindstrom (1963) in the Swedish Ordovician.

Tops of many lime mudstone mounds are sites of discontinuity surface development. Similar meandering burrows are present and may be more abundant than in other types of truncation surfaces. These mound-crest surfaces are commonly surrounded by encrinites as well. Commonly, though not consistently, such encrinites contain pebbles identical in lithology to the underlying mounds. These pebbles tend to be larger around larger mounds, are frequently iron-stained, and are usually angular and blocky.

Surfaces of reefs and surrounding lime mudstone are truncated or eroded, as evidenced by individual truncation of sponges and *Calathium*. Morphologies change markedly upward from approximately 10 cm above the bases of the reefs. Surfaces are smooth below reef margins, but about 10 cm above the reef base truncated surfaces have textures dominated by overlapping bowl-

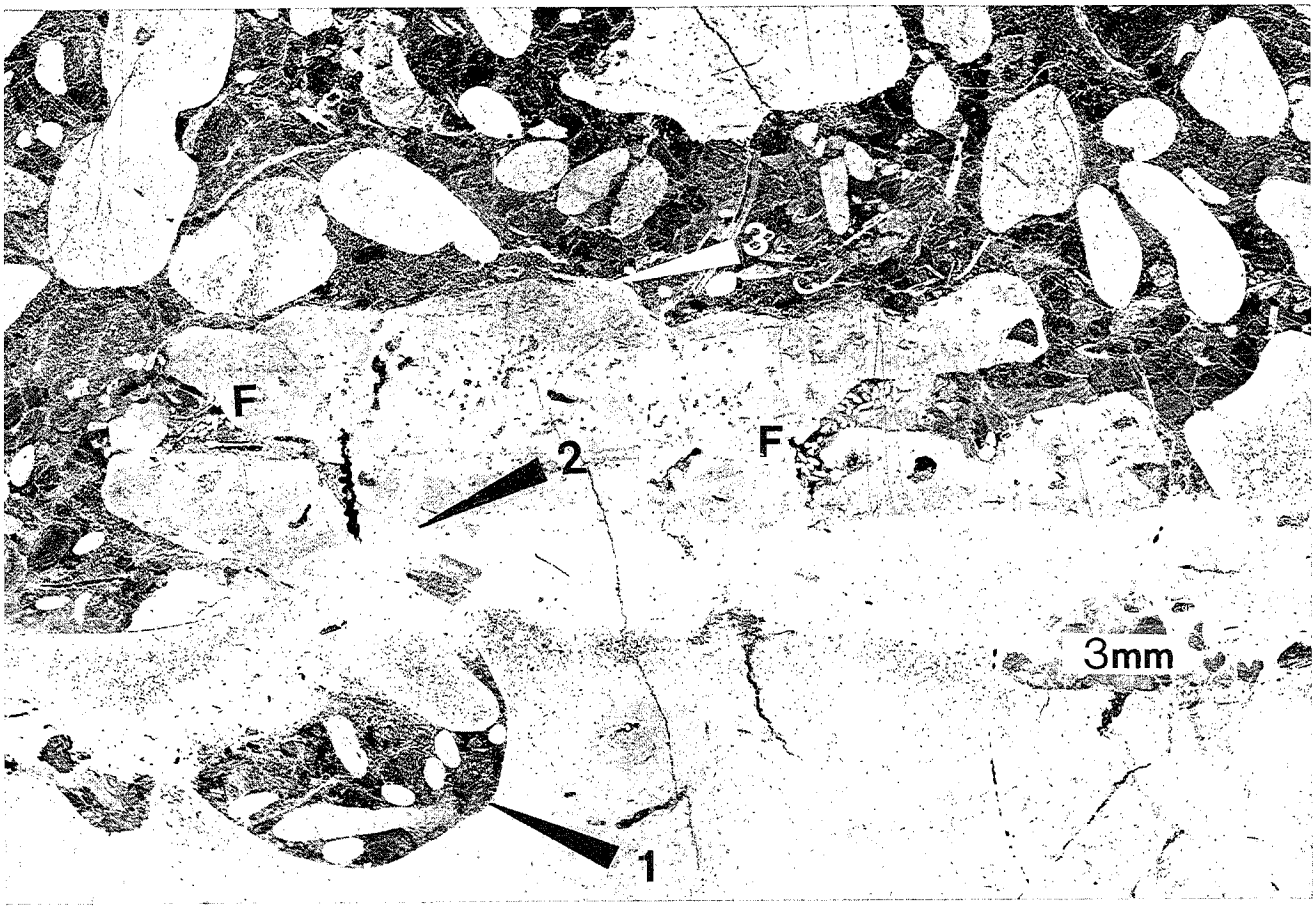

FIGURE 26.—*Projection print from peel of hardground showing typical development on lime mudstone substrate with associated encrinite. Note fine preservation of fecal pellets (F) in cavities on the surface and three generations of hardgrounds (1–3). Outcrop near section 1 approximately at the 25-m level.*

shaped depressions bounded by relatively sharp corners (fig. 32). Some smooth horizontal parts of the surface near the reef bases form small, flat-bottomed enclosed basins that undercut the reef slightly. These features are reminiscent of solution rock pools influenced by meteoric solution reported by Esteban and Klappa (1983) from the Yucatán Peninsula. They also strongly resemble the intertidal area of the rocky coasts of Andros Island as described by Donn and Boardman (1988). Here the terrace, nip, and escarpment are analogous with the reef pool, undercut, and main reef surface, respectively. In the Bahamas the characteristic pitting has been attributed to bioerosion by chitons (Donn and Boardman 1988). Such pitting can occur subtidally (Neumann 1966), but intertidal exposure of the reef surface has not been ruled out. The iron-stained silicified crust of the reef horizon is up to 1 cm thick at the top of the reefs and thins progressively to about 1 mm thick around reef bases.

Fossils

Hardground communities are generally taphonomically altered by condensation and "cannibalism" from reworking. However, the presence of occasional whole, well-preserved echinoderm fossils indicates that some echinoderms did live in this environment. Like hardgrounds from other formations (Goldring and Kazmierczak 1974, Koch and Strimple 1968), well-preserved echinoderms occasionally occur in encrinite deposits on hardgrounds. Church (1974) reported one such occurrence on top of a reef. During this study there were two similar finds. One cystoid was found on a pebble pavement at 87.7 m, and a crinoid calyx was found at 77.0 m. Numerous other hardgrounds have some articulated ossicles, pelma, or arm fragments.

Environmental Interpretation

A scenario for formation of hardgrounds has been presented by Aigner (1985), Einsele (1982), and Seilacher (1982). They suggested that where coarse storm deposits overlie lime mud or shale, pore water circulates to lithify the subadjacent lime mud or shale. The lithified mudstone is termed an *underbed.* Subsequent storms ex-

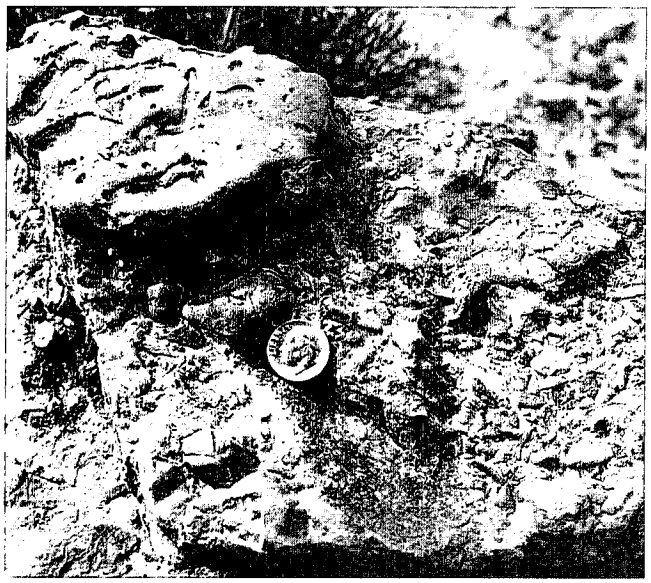

FIGURE 27.—*Bedding plane view of low-relief hardground on lime mudstone. Below section 5 at approximately the 25-m level of section 1.*

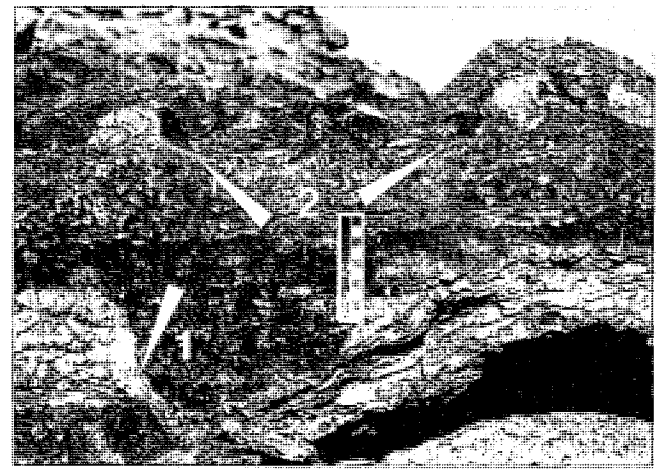

FIGURE 28.—*Horizontal view of outcrop of two different discontinuity surfaces (1–2). Upper surface is a hardground with moderate relief and a well-defined reddish brown stain. Lower surface is a discontinuity surface developed on lime mud mounds. Section 1 at 42.6 m.*

humed and reworked underbeds, breaking them up and forming intraclasts or exposing them on the sea floor as hardgrounds. Fillmore encrinites resulted from reworking and are often associated with hardgrounds. This association is compatible with a causal relationship between reworking and hardground formation and indicates that thin lime mudstone underbeds are genetically different from the much thicker, dense lime mudstone beds. This mechanism functions subtidally at a maximum depth near fair-weather wave base.

Some units, such as the reef lime mudstone at 19.6 m in section 1, may have been lithified or at least bound very soon after formation, and the reef horizon at 33.5 m was not likely to have ever been entirely covered by a single storm deposit. These hardgrounds could have formed here by unmediated exposure to cementing fluids and may have formed intertidally as well as subtidally or below wave base.

STORM DEPOSITIONAL MODEL

Development of the Model

During onset and culmination of storms, sea bottoms may be scoured, large clasts may be sorted, and fine-grained sediments are suspended (Kreisa 1981, Kreisa and Bambach 1982, Seilacher 1982). As storms wane, sediment is rapidly redeposited (Kreisa and Bambach 1982, Seilacher 1982). If this takes place with little or no lateral transport, the resultant sequence consists of (1) a sharp, erosional base; (2) a normally graded basal pebble or shell lag; (3) planar-laminated arenite; (4) wave-rippled arenite; and (5) planar-laminated mud that grades into overlying pelagic shale (Aigner 1982, Kreisa 1981, Seilacher 1982).

Storm deposits nearly always differ from the ideal because lateral transport is significant, commonly resulting from seaward rip currents that compensate for nearshore water buildup (Kreisa and Bambach 1982, Seilacher 1982). Erosion and suspension occur landward (proximally), and rapid deposition occurs seaward (distally).

Figure 33 is a simplified representation of a storm depositional model for the Fillmore based largely on summary figures by Aigner (1985, figs. 1 and 49) and Kreisa and Bambach (1982, fig. 1), combined with specific characteristics of the Fillmore Formation. This model differs from the generalized Aigner and the Kreisa and Bambach diagrams in that it (1) does not attempt to represent all lithologies encountered in the study, and (2) it shows only one or two lithologies per event deposit in any one place, to reflect the states of actual event deposit observed in the Fillmore.

It is also important to note that the Aigner and the Kreisa and Bambach models are based on bioclastic limestones rather than on intraformational conglomerates.

FILLMORE STORM DEPOSITS

Figure 33 illustrates three basic types of storm deposits as found in the study interval: (1) encrinites; (2) trilobite-dominated flat-pebble conglomerates; and (3) planar-laminated calcarenites and calcisiltites. The figure relates these lithologies to decreasing proximality and increasing depth along a single storm bed. But fair-weather sedimentation rate; local sedimentary characteristics; and

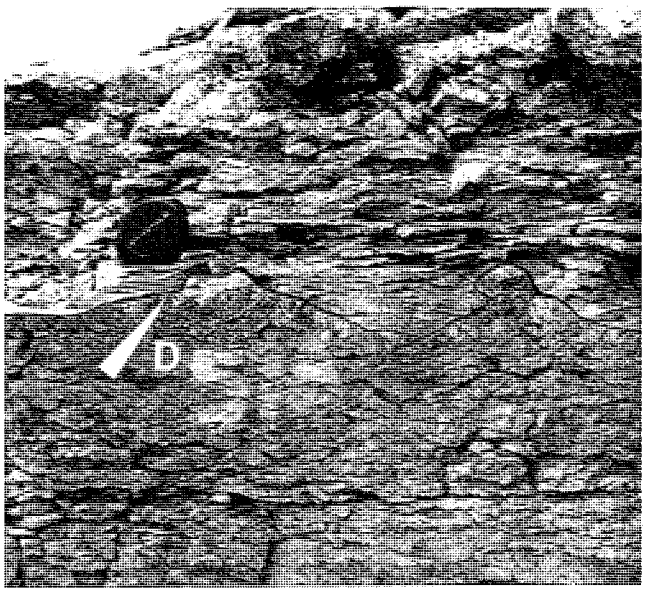

FIGURE 29.—*Horizontal view of outcrop of discontinuity surface (D) on lime mudstone of moderate relief without significant development of reddish brown stain. Section 3 at 51.8 m. Camera lens cap for scale.*

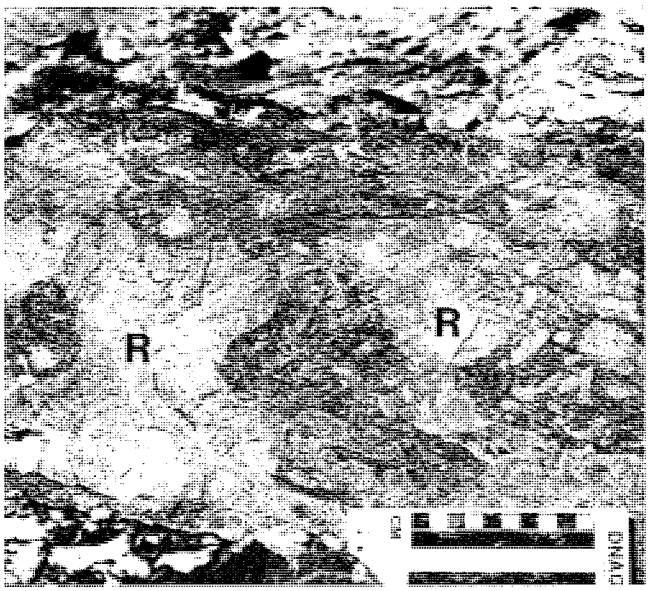

FIGURE 30.—*Outcrop of high-relief hardground developed on reef lime mudstone (R) shows definite mushroom-shaped pillars and coarse, angular, locally derived lithoclasts. Section 1 at 19.7 m.*

FIGURE 31.—*Hardground surface shows typical borings that have been truncated by subsequent erosion. Photograph of hand sample from section 1 at 42.6 m.*

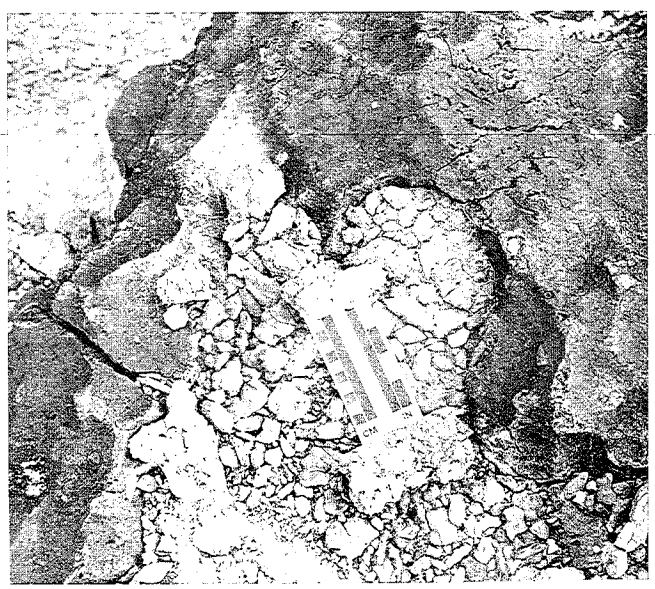

FIGURE 32.—*Bedding plane view of reef (studied by Church [1974]) shows thick rind and surface texture similar to that developed in limestones that have undergone intertidal exposure in humid tropical climates. Section 1 at 33.9 m.*

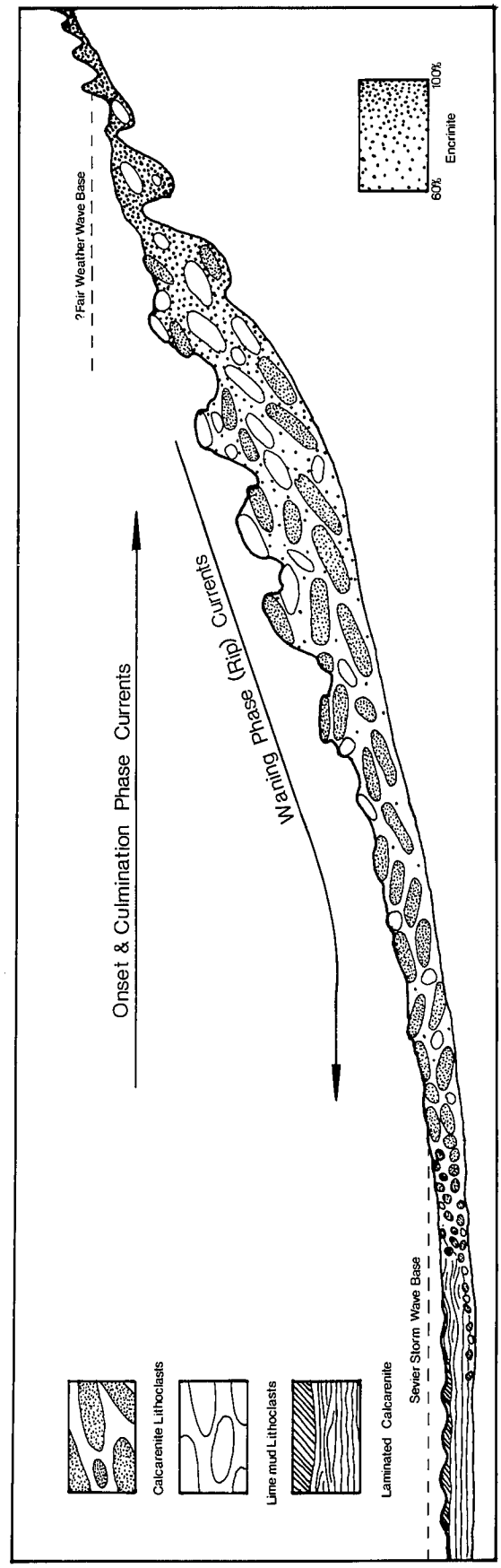

FIGURE 33.—*Simplified diagram of storm deposits interpreting relationships between storm currents, water depth, and composition of flat-pebble conglomerates and calcisiltite-calcarenites. Slope much exaggerated.*

storm frequency, violence, direction, and location along strike all influence the effects of a given event.

Encrinite units were reworked by multiple storms and fair-weather shoaling, which winnowed fines and abraded clasts. Less durable trilobite and brachiopod grains as well as some intraclasts were destroyed.

Trilobite-dominated flat-pebble conglomerate beds were each formed by a single to a few storms in shallow subtidal waters. Each event scoured the bottom and ripped up moderately to well-lithified calcisiltite lithoclasts that were transported short distances distally by waning-phase rip currents and mixed with more proximally derived lime-mud clasts upon resettling. Skeletal fragments of trilobites were exhumed from shale and retained this mud matrix in hollows of spines and tight folds as they resettled on, and infiltrated between, previously deposited lithoclasts.

Calcisiltites and fine calcarenites were formed at or below storm wave base and formed as waning-phase currents deposited finer-grained suspended material. As these currents slowed down they occasionally left tool marks in the underlying mud and a succession of planar-laminated, hummocky cross-stratified, and ripple-laminated deposits.

Trilobite packstones, not figured in the diagram, probably result from storm winnowing of deeper-water, shale-dominated environments.

CURRENT DIRECTIONS

Paleocurrent data are consistent with the storm interpretation. Imbrication, cross-bedding, and other current indicators measured in the field are plotted on rose diagrams in figure 34. Resultant vectors were determined and statistically validated with the Rayleigh test of significance described by Curray (1956). These vectors are shown only if significant at a 5% confidence interval.

The first of the five rose diagrams, termed *unimodal,* represents imbrications from flat-pebble conglomerate beds with one current direction. The second, termed *bimodal,* is from flat-pebble conglomerate beds with two different current directions in each bed. The third is a total of the first two, and the fourth includes only trilobite-dominated flat-pebble conglomerates. The fifth, termed *calcarenite,* includes all current-direction indications from calcisiltite-calcarenite beds, such as those from sole markings and ripple crests.

Multidirectionality, which causes the apparent random distribution of some diagrams, can indicate storm influence on a level subtidal bottom (Whisonant 1987).

Flat-pebble conglomerates with unimodal currents show a statistically significant northwest trend, parallel to the Ordovician shoreline. This could be the result of coastally deflected onshore flow during storms.

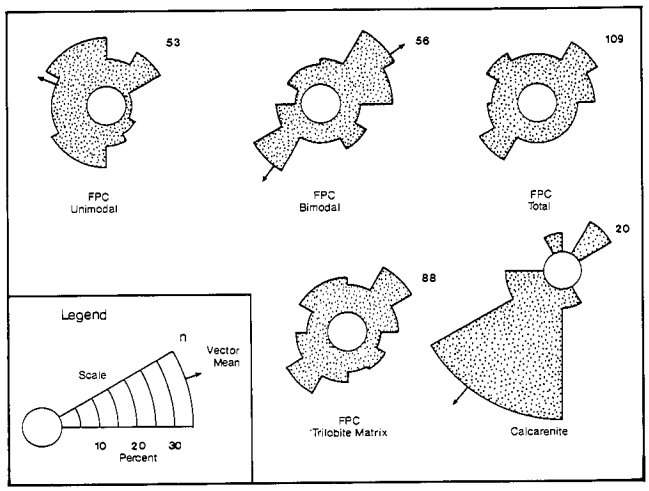

FIGURE 34.—*Rose diagrams represent current indicators from flat-pebble conglomerate and calcisiltite-calcarenite beds. FPC = flat-pebble conglomerate. FPC unimodal: beds with one current direction each; FPC bimodal: beds with two current directions; FPC total: sum of unimodal and bimodal beds; FPC trilobite matrix: all trilobite-dominated flat-pebble conglomerate current readings; and calcarenite: all calcisiltite and calcarenite beds. See text for full explanation.*

The northeast and southwest bimodal tendency, visible in all of the diagrams, is onshore-offshore parallel to the trend of the Ibex basin and resulted from storm tidal currents, summarized in figure 33. Bimodal beds have more consistent current directions than unimodal beds. Their dominant mode is shoreward, and consistency of current readings from bimodal beds may be due to proximity to shore, as reported from other formations (Lindholm 1980, Whisonant 1987). Figure 33 shows that shoreward imbrication is expected to form during onset and culmination of a storm and would not be present in deeper-water deposits. The trend of the reef horizon at 33.5 m (N 31 E) parallels the bimodal storm-current tendency. This is a consistent relationship in both ancient and modern reefs (Ball and others 1967, James 1983, Pratt and James 1982) and may result from storm damage that restricts reef growth in hydrodynamically unstable orientations.

The clear offshore trend in calcisiltite-calcarenite beds reflects the tendency of waning-phase rip currents to transport finer-grained material seaward (Kreisa and Bambach 1982).

CYCLIC SEDIMENTATION AND BATHYMETRY

Stratigraphic sequence and lithologic association provide keys to understanding the relationship between demonstrable tempestite lithologies discussed above and "fair-weather" deposits such as shale, wavy-laminated lime mudstone, and dense lime mudstone. In figure 35,

which is a stratigraphic column representing section 1, inverted triangles represent interpreted shoaling-upward cycles (compare fig. 4). The general pattern of succession and lithologic association within a cycle is (1) a basal thick shale with thin beds of calcisiltite-calcarenite, trilobite-dominated flat-pebble conglomerate, and trilobite packstone; (2) a middle interval dominated by wavy-laminated lime mudstone with trilobite-dominated flat-pebble conglomerates and some encrinite units; and (3) an upper zone of encrinite units with associated hardgrounds and lime mudstone mounds interbedded with shale, wavy-laminated lime mudstone and dense lime mudstone.

These cycles resulted from fluctuations in water depth and provide evidence for the total range of relative sea-level change in this area. Intercalated storm lithologies serve to limit depth interpretations of fair-weather units. Based on the presence of trilobite packstones, calcisiltites, and flat-pebble conglomerates in thicker shale intervals, water depth during shale deposition in the study interval did not greatly exceed severe storm wave base, which in modern seas is close to a 50-m depth. Wavy-laminated lime mudstone, which may be tidally influenced, was deposited above severe storm wave base, whereas mounded lime mudstone, with closely associated hardgrounds and encrinite flat-pebble conglomerates, was formed close to fair-weather wave base. Biostromal lime mudstone, with its rhythmic alternation of spiculite, lime-mud and silt laminae, and its few very thin lithoclastic encrinite beds, could have resulted from intertidal or supratidal deposition in a tidal-flat environment.

Two magnitudes of cycles are shown on the diagram. The smaller cycles, 2 to 4 m thick, tend to contain a limited range of lithologies. Using Walther's law, each such cycle can be thought of as a sample along an offshore-onshore transect of a single-cycle deposit. For example: (1) offshore, near storm wave base, 12.1 to 14.9 m is dominated by shale and contains some calcisiltite-calcarenites, trilobite-dominated and encrinite-dominated flat-pebble conglomerates, and one discontinuity surface at the top; (2) offshore, above storm wave base, 26.9 to 30.6 m is dominated by shale and trilobite-dominated flat-pebble conglomerates and contains encrinites, hardgrounds, and some wavy-laminated lime mudstone near the top; (3) close to fair-weather wave base, 30.6 to 33.6 m is dominated by shale and wavy-laminated lime mudstone and is capped by a sponge-algal mound and hardground with encrinite; and (4) intertidal to supratidal, 45.5 to 47.5 m is dominated by dense lime mud containing a few encrinite stringers and is capped by a hardground.

Larger cycles 7 to 12 m thick demonstrate the same general pattern of upward shoaling with a wider range of component lithologies. Section 1 is composed of parts of two larger shoaling-upward cycles, shown by the two pages of figure 35. The shallowest part of this section is at 47.5 m, the break between these two cycles.

Overall, there is a marked decrease in shale content toward the top of the section, which probably results from overall shallowing. This trend may reflect a larger scale cyclicity.

DEPOSITIONAL ENVIRONMENT

Lithologic associations and stratigraphic sequence were used to construct figure 36, a block diagram summarizing the depositional environment across the upper part of one small-scale cycle at low tide. The shoaling upward sequence is reflected in the block diagram by the shoreward progression from shale to lime mud. The associations between storm deposits and fair-weather microfacies are reflected in the placement of two storm-deposit sheets—one represented at the sediment-water interface, and another below, exposed in the cutaway side of the block. Each sheet consists of a deep, distal calcisiltite-calcarenite; an intermediate trilobite-dominated flat-pebble conglomerate; and a shallow proximal encrinite. The buried sheet shows a continuation into the intertidal biostromal lime mud. This continuation represents a spillover deposit of finer lithoclasts and encrinite.

Sponge-algal reefs only occur at two horizons within the study interval but are included in this diagram because several similar intervals occur both above and below in the Fillmore. Two examples are included in the diagram. One group, modeled after the horizon at 33.5 m in section 1 studied by Church (1974), is placed in the subtidal zone below normal wave base and shows, schematically, smooth, unaltered surfaces of several elongate reefs. The reefs are aligned with the same strong currents that left megaripples in the exposed storm deposit. The second reef example shows how the same reef appears after corrasion in the intertidal zone.

The diagram is not to scale because lateral distances are larger than the largest space between measured sections; changes in single beds over 500-m distance were noted on the order of a percentage change in echinoderm content, or change in pebble content, but never spanned a fundamental change in environment. The width of the block is about 30 to 40 m. The length from low tide offshore is at least 5 km and may be as many as 20 km or more, based on lengths of reef outcrops reported by Church (1974). Maximum depth is close to severe storm wave base, which may be about 50 m.

CONCLUSIONS

A middle interval of the Fillmore Formation was deposited on a passive margin in marine environments that ranged from below storm wave base, at least 30 m deep, to

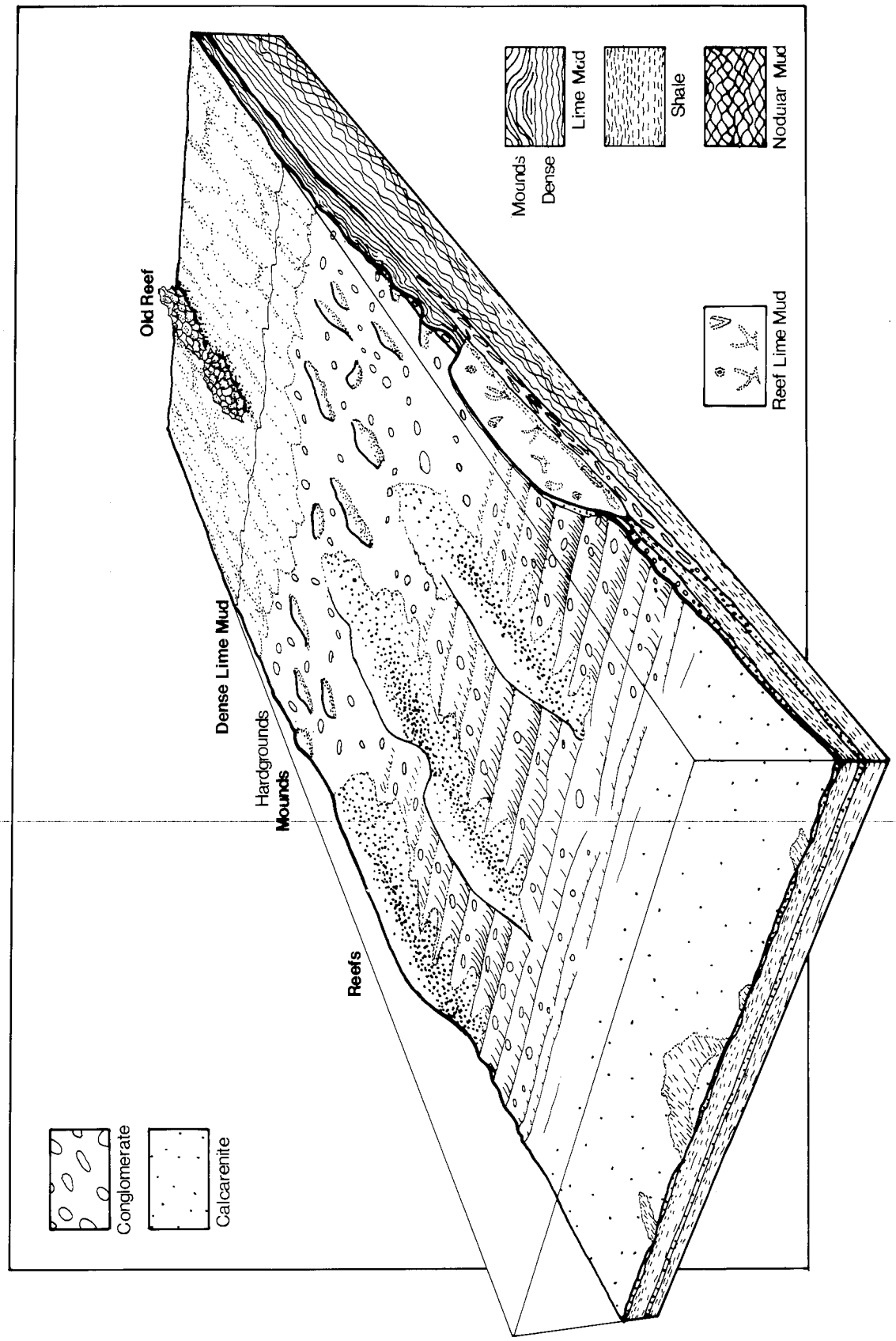

FIGURE 36.—*Block diagram showing a conceptual model of deposition for this part of the Fillmore Formation at low tide. Not to scale.*

possibly supratidal. The section records several shoaling-upward cycles 2 to 4 m thick. These consist, from bottom to top, of (1) shale with interbedded trilobite packstones, calcisiltites, calcarenites, and trilobite-dominated flat-pebble conglomerates; (2) wavy-laminated lime mud, calcisiltite, and shale with interbedded calcisiltites, calcarenites, flat-pebble conglomerates, and encrinites with hardgrounds; and (3) interlaminated algal lime mudstone and calcisiltite with sparse encrinite and hardgrounds.

Fossil assemblages change gradually between shale and lime mudstone. Shale assemblages contain a variety of trilobites, graptolites, cephalopods, sponges, gastropods, brachiopods, and small, horizontal deposit-feeder burrows. The assemblage is indicative of quiet, normal marine conditions. Lime mudstone assemblages are dominated by large asaphid trilobites, high-spired gastropods, and large horizontal and vertical burrows, indicating a shallow-water environment.

Thin and very thin interbedded calcisiltite, calcarenite, flat-pebble conglomerate grainstone, and packstone and encrinite grainstone are interpreted as storm deposits.

Planar-laminated calcisiltite beds average 3 to 5 cm thick. Bioturbation is concentrated near tops of beds, and escape structures are common. Some calcisiltite-calcarenite beds contain chert nodules that do not interrupt internal lamination but are about twice as thick as the bed, suggesting differential compaction. Calcisiltite-calcarenites are commonly lateral equivalents of flat-pebble conglomerate beds and are best developed as interbeds in shale. Current directions interpreted from sole markings and ripple lamination are oriented strongly southwest in calcisiltite-calcarenite units, parallel to the axis of the Ibex basin.

Intraclastic limestones consist of calcisiltite and lime mud lithoclasts in matrix dominated by echinoderm fragments, trilobite fragments, or lime mud and silt. These beds thin and pinch out over distances of less than 100 m. Matrix forms infiltration structures, which are especially well developed in trilobite- and lime mud–dominated matrix. Current directions, interpreted from imbrication and megaripples, are bimodal in a northeast-southwest direction, parallel to the axis of the Ibex basin in which these rocks were deposited. These and other coarse lithologies formed as storm-generated, high-velocity oscillatory currents ripped up and reworked bottom sediment, forming coarse bio- and lithoclastic lags. Water piled onshore during storm culmination, producing shoreward intraclast imbrication, but reversed clast orientation during storm waning. Intraclastic limestones were deposited in shallow subtidal waters. Those enriched in echinoderm debris were likely deposited in somewhat shallower waters.

Other lithologies are also storm generated. Calcisiltite-calcarenite was deposited distally below storm wave base by waning-phase rip currents. Trilobite packstones were formed by winnowing of trilobite-rich mud in deep water.

Loaf-shaped sponge-algal mounds, up to 1 m across and high and several meters long, are spaced at 10-m intervals in the reef horizon and consist of microbial-bound lime mudstone. They are aligned parallel to bimodal storm-bed current direction (perpendicular to ripple crests) and were probably influenced by storm currents, much like modern digitate reefs (James 1983). They occur stratigraphically at 100-m intervals and have pitted, scalloped surfaces, which suggests the possibility that they were exposed intertidally after growth.

These reefs contain a diverse fauna of sponges, algae, brachiopods, echinoderms, gastropods, and cephalopods. This assemblage suggests reef formation in open-marine conditions and clear water.

Hardgrounds formed on a variety of substrates. They commonly have a ferruginous silicified rind and show truncation of underlying sediments. They are developed on flat-pebble conglomerates, ripple-carved flat-pebble conglomerates, truncated calcisiltite, lime mudstone surfaces, lime mudstone mound surfaces, and surfaces of large reefs.

Most hardgrounds formed through action of repeated storms on the sea bottom. Development usually began with lithification of lime muds and silts a short distance below the substrate. Storms exhumed and broke up the lithified layers and incorporated intraclasts into conglomerates. These were often buried, relithified, and exhumed. Repeated storms failed to rework the lithified horizon and resulted in cannibalization of the original storm deposit. Eventually the hardground surface was locally exposed and colonized. Some hardgrounds may have formed from algal-bound sediments in turbulent, carbonate-rich environments. Hardground assemblages are dominated by encrusting echinoderms, such as crinoids and rhombiferans.

REFERENCES CITED

Aigner, T., 1982, Calcareous tempestites: storm dominated stratification in Upper Muschelkalk Limestones (Middle Trias, SW-Germany): In Einsele, G., and Seilacher, A. (eds.), Cyclic and event stratification: Springer-Verlag, New York, p. 180–98.

———, 1985, Storm depositional systems: In Friedman, G. M., Neugebauer, H. J., and Seilacher, A. (eds.), Lecture notes in earth science, no. 3: Springer-Verlag, New York, 174p.

Aitken, J. D., 1967, Classification and environmental significance of cryptalgal limestones and dolomites, with illustrations from the Cambrian and Ordovician of southwestern Alberta: Journal of Sedimentary Petrology, v. 37, p. 1163–78.

Ball, M. M., Shinn, E. A., and Stockman, K. W., 1967, The geologic effects of Hurricane Donna in south Florida: Journal of Geology, v. 75, p. 583–97.

Berry, W. B. N., 1962, Comparison of some Ordovician limestones: American Association of Petroleum Geologists Bulletin, v. 46, p. 1701–20.

Braithwaite, L. F., 1976, Graptolites from the Lower Ordovician Pogonip Group of western Utah: Geological Society of America, Special Paper 166, 106p.

Bromley, R. G., 1975, Trace fossils at omission surfaces: In Frey, R. W. (ed.), The study of trace fossils: Springer-Verlag, New York, p. 399–428.

Church, S. B., 1974, Lower Ordovician patch reefs in western Utah: Brigham Young University Geology Studies, v. 21, pt. 3, p. 41–62.

Cressman, E. R., and Noger, M. C., 1976, Tidal-flat carbonate environments in the High Bridge Group (Middle Ordovician) of central Kentucky: University of Kentucky, Kentucky Geological Survey, Series X, Report of Investigations 18, p. 1–15.

Curray, J. R., 1956, The analysis of two-dimensional orientation data: Journal of Geology, v. 64, p. 117–31.

Demeter, E. J., 1973, Lower Ordovician pliomerid trilobites from western Utah: Brigham Young University Geology Studies, v. 20, pt. 4, p. 37–65.

Donn, T. F., and Boardman, M. R., 1988, Bioerosion of rocky carbonate coastlines on Andros Island, Bahamas: Journal of Coastal Research, v. 4, no. 3, p. 381–94.

Droser, M. L., and Bottjer, D. J., 1986, A semiquantitative field classification of ichnofabric: Journal of Sedimentary Petrology, v. 56, no. 4, p. 558–59.

Einsele, G., 1982, Limestone-marl cycles (periodites): Diagnosis, significance, causes a review: In Einsele G., and Seilacher, A. (eds.), Cyclic and event stratification: Springer-Verlag, New York, p. 8–53.

Esteban, M., and Klappa, C. F., 1983, Subaerial exposure environment: In Scholle, P. A., et al. (eds.), Carbonate depositional environments: American Association of Petroleum Geologist, Memoir 33, p. 1–95.

Ethington, R. L., and Clark, D. L., 1981, Lower and Middle Ordovician conodonts from the Ibex area, western Millard County, Utah: Brigham Young University Geology Studies, v. 28, pt. 2, 155p.

Futterer, E., 1982, Experiments on distinction of wave and current influenced shell accumulations: In Einsele, G., and Seilacher, A. (eds.), Cyclic and event stratification: Springer-Verlag, New York, p. 175–79.

Goldring, R., and Bridges, P. H., 1973, Sublittoral sheet sandstones: Journal of Sedimentary Petrology, v. 43, p. 736–47.

Goldring, R., and Kazmierczak, J., 1974, Ecological succession in intraformational hardground formation: Paleontology, v. 17, no. 4, p. 949–62.

Hardie, L. A., and Ginsburg, R. M., 1977, Layering: The origin and environmental significance of lamination and thin bedding: In Hardie, L. A. (ed.), Sedimentation on the modern tidal flats of Northwest Andros Island, Bahamas: The Johns Hopkins University Press, Baltimore, p. 50–123.

Hintze, L. F., 1951, Lower Ordovician detailed stratigraphic sections for western Utah and eastern Nevada: Utah Geological and Mineralogical Survey, Bulletin 39, 99p.

———, 1973, Lower and Middle Ordovician stratigraphic sections in the Ibex area, Millard County, Utah: Brigham Young University Geology Studies, v. 20, pt. 4, p. 3–36.

———, 1974a, Preliminary geologic map of the Barn Quadrangle, Millard County, Utah: U.S. Geological Survey, Miscellaneous Field Studies MF 633, scale 1:48,000.

———, 1974b, Preliminary geologic map of the Notch Peak Quadrangle, House Range, Millard County, Utah: U.S. Geological Survey, Miscellaneous Field Studies MF 636, scale 1:48,000.

James, N. P., 1983, Reef environment: In Scholle, P. A., et al. (eds.), Carbonate depositional environments: American Association of Petroleum Geologists, Memoir 33, p. 345–462.

Jensen, R. G., 1967, Ordovician brachiopods from the Pogonip Group of Millard County, western Utah: Brigham Young University Geology Studies, v. 14, p. 67–100.

Kahle, C. F., 1965, Possible roles of clay minerals in the formation of dolomite: Journal of Sedimentary Petrology, v. 35, p. 448–53.

Kennard, J. M., and James, N. P., 1986, Thrombolites and stromatolites: Two distinct types of microbial structures: Palaios, v. 1, p. 492–503.

Knouth, L. P., 1979, A model for the origin of chert in limestone: Geology, v. 7, p. 274–77.

Koch, D. L., and Strimple, H. L., 1968, A new Upper Devonian cystoid attached to a discontinuity surface: Iowa Geological Survey Report of Investigations 5, 50p.

Kreisa, R. D., 1981, Storm-generated sedimentary structures in subtidal marine facies with examples from the Middle and Upper Ordovician of southwest Virginia: Journal of Sedimentary Petrology, v. 51, p. 823–48.

Kreisa, R. D., and Bambach, R. D., 1982, The role of storm processes in generating shell beds in the Paleozoic shelf environments: In Einsele, G., and Seilacher, A. (eds.), Cyclic and event stratification: Springer-Verlag, New York, p. 200–207.

Laporte, L. F., 1969, Recognition of a transgressive carbonate sequence within an epeiric sea: Helderberg Group (Lower Devonian) of New York State: In Friedman, G. M. (ed.), Depositional environments in carbonate rocks: Society of Economic Paleontologists and Mineralogists, Special Publication 14, p. 98–118.

Lee, Y. I., and Friedman, G. M., 1987, Deep-burial dolomitization in the Ordovician Ellenburger Group carbonates, western Texas and southeastern New Mexico: Journal of Sedimentary Petrology, v. 57, p. 544–57.

Lindholm, R. C., 1980, Intraclast orientation in Cambro-Ordovician limestones in western Maryland: Journal of Sedimentary Petrology, v. 50, p. 1205–12.

Lindstrom, M., 1963, Sedimentary folds and the development of limestone in an Early Ordovician sea: Sedimentology, v. 2, p. 243–92.

Markello, J. R., and Read, J. F., 1981, Carbonate ramp to deeper shale-shelf transitions of an Upper Cambrian intrashelf basin, Nolichucky Formation, southwest Virginia Appalachians: Sedimentology, v. 28, p. 573–97.

———, 1982, Upper Cambrian intrashelf basin, Nolichucky Formation, southwest Virginia Appalachians: American Association of Petroleum Geologists Bulletin, v. 66, p. 860–78.

Neumann, A. C., 1966, Observations on coastal erosion in Bermuda and measurements of the boring rate of the sponge *Cliona lampa:* Limnology and Oceanography, v. 11, p. 92–108.

Osmond, J. C., 1963, Ripple marks cut on Ordovician limestone pebble conglomerates, Stansbury Range, Utah: Journal of Sedimentary Petrology, v. 33, no. 1, p. 105–11.

Palmer, T. J., and Fursich, F. T., 1974, The ecology of a Middle Jurassic hardground and crevice fauna: Palaeontology, v. 17, no. 3, p. 507–24.

Pratt, B. R., 1982, Stromatolitic framework of carbonate mudmounds: Journal of Sedimentary Petrology, v. 52, p. 1203–27.

Pratt, B. R., and James, N. P., 1982, Cryptalgal-metazoan bioherms of early Ordovician age in the St. George Group, western Newfoundland: Sedimentology, v. 29, p. 543–69.

———, 1986, The St. George Group (Lower Ordovician) of western Newfoundland: Tidal flat island model for carbonate sedimentation in shallow epeiric seas: Sedimentology, v. 33, p. 313–43.

Rhoads, D. C., 1975, The paleoecological and environmental significance of trace fossils: In Frey, R. W. (ed.), The study of trace fossils: Springer-Verlag, New York, p. 147–60.

Seilacher, A., 1982, General remarks about event deposits: In Einsele, G., and Seilacher, A. (eds.), Cyclic and event stratification: Springer-Verlag, New York, p. 161–73.

Sepkoski, J. J., Jr., 1982, Flat-pebble conglomerates, storm deposits, and the Cambrian bottom fauna: In Einsele, G., and Seilacher, A. (eds.), Cyclic and event stratification: Springer-Verlag, New York, p. 371–85.

Shinn, E. A., Lloyd, R. M., and Ginsburg, R. N., 1969, Anatomy of a modern carbonate tidal flat, Andros Island, Bahamas: Journal of Sedimentary Petrology, v. 39, p. 1202–28.

Stewart, J. H., and Poole, F. G., 1974, Lower Paleozoic and uppermost Precambrian Cordilleran miogeocline, Great Basin, Western United States: In Dickinson, W. R. (ed.), Tectonics and sedimentation: Society of Economic Paleontologists and Mineralogists, Special Publication 22, p. 28–57.

Wilson, J. L., 1975, Carbonate facies in geologic history: Springer-Verlag, New York, 471p.

Whisonant, R. C., 1987, Paleocurrent and petrographic analysis of imbricate intraclasts in shallow-marine carbonates, Upper Cambrian, southwestern Virginia: Journal of Sedimentary Petrology, v. 57, no. 6, p. 983–94.